remote sensing

MDPI

Article

A New Compact Delay, Doppler Stretch and Phase Estimation CRB with a Band-Limited Signal for Generic Remote Sensing Applications

Priyanka Das [1,2], Jordi Vilà-Valls [1,*], François Vincent [1], Loïc Davain [2] and Eric Chaumette [1]

[1] Institut Supérieur de l'Aéronautique et de l'Espace, University of Toulouse, 31055 Toulouse, France; priyanka.das@isae-supaero.fr (P.D.); francois.vincent@isae-supaero.fr (F.V.); eric.chaumette@isae-supaero.fr (E.C.)

[2] Safran/Sagem DS, 95610 Eragny, France; loic.davain@safrangroup.com

* Correspondence: jordi.vila-valls@isae-supaero.fr

Received: 22 July 2020; Accepted: 2 September 2020; Published: 8 September 2020

Abstract: Since time-delay, Doppler effect and phase estimation are fundamental tasks in a plethora of engineering fields, tractable lower performance bounds for this problem are key tools of broad interest for a large variety of remote sensing applications. In the large sample regime and/or the high signal-to-noise ratio regime of the Gaussian conditional signal model, the Cramér–Rao bound (CRB) provides an accurate lower bound in the mean square error sense. In this contribution, we introduce firstly a new compact CRB expression for the joint time-delay and Doppler stretch estimation, considering a generic delayed and dilated band-limited signal. This generalizes known results for both wideband signals and the standard narrowband signal model where the Doppler effect on the band-limited baseband signal is not considered and amounts to a frequency shift. General compact closed-form CRB expressions for the amplitude and phase are also provided. These compact CRBs are expressed in terms of the baseband signal samples, making them especially easy to use whatever the baseband signal considered, therefore being valid for a variety of remote sensors. The new CRB expressions are validated in a positioning case study, both using synthetic and real data. These results show that the maximum likelihood estimator converges to the CRB at high signal-to-noise ratios, which confirms the exactness of the CRB. The CRB is further validated by comparing the ambiguity function and its 2nd order Taylor expansion where the perfect match also proves its exactness.

Keywords: time-delay; Doppler effect and phase estimation; Cramér–Rao bound; maximum likelihood; band-limited signals; GNSS remote sensing

1. Introduction

Time-delay, Doppler stretch and phase estimation appear in a plethora of engineering fields such as navigation, radar, reflectometry, sonar or communications, to name a few [1–12], being the estimation of such parameters a key first stage of the receiver [7,10–12]. For any of these applications, when designing and assessing estimation techniques, it is of fundamental importance to know the ultimate achievable performance in the mean square error (MSE) sense, information which can be brought by lower bounds (LB) on the MSE. Even if several types of LBs exist [13], the family of Cramér–Rao bounds (CRB) [14,15] is the most popular, mainly due to its simplicity of calculation for various problems (see [6] (§8.4) and [13] (Part III)). In addition, the CRB gives an accurate estimation of the MSE of the maximum likelihood estimator (MLE) in the asymptotic region of operation under certain conditions, i.e., in the large sample regime and/or high signal-to-noise

(SNR) regime of the Gaussian conditional signal model (CSM) [16,17]. Therefore, it is not surprising that several CRB expressions for the delay-Doppler estimation problem have been derived for the past decades, for finite [4,18–32] or infinite [33] bandwidth signals, where the starting point is often either the Slepian–Bangs formulas [15] or general theoretical CRB expressions for Gaussian observation models [6,34–36].

Most of these CRB expressions [4,20,21,23–27,31,32] only address the standard narrowband signal model where the impact of the Doppler effect on the baseband signal is not taken into account and amounts to a frequency shift. However, in some applications [3,7,29], like wide/ultra-wide band (high range resolution, synthetic aperture or low interception probability) sonar or radar, or wide/ultra-wide band communications, the compression or stretch due to the range rate on the envelope of the received signal cannot be ignored. In radar, the standard narrowband signal model was first proposed by Woodward [1] for deterministic transmit waveforms and led to the conventional narrowband range-Doppler MLE and its associated narrowband radar ambiguity function. Following Woodward's approach, various formulations for the wideband range-Doppler MLE and its associated ambiguity function were later investigated [2,3,7,37–39], and the significance of the difference between the two ambiguity functions has been shown to depend on the product of the signal duration, the signal bandwidth, and the target velocity [3]. In addition to the historical remote sensing systems as sonar and radar, in more recent Global Navigation Satellite Systems (GNSS), due to the very high velocity of the transmitter located on a satellite, it is also essential to incorporate the baseband signal dilatation due to the Doppler effect into the MLE formulation to reach the minimum achievable MSE, for instance in carrier phase-based precise positioning techniques [40]. In addition, this is also the case of GNSS-based reflectometry (GNSS-R) applications such as altimetry [12,41,42].

Surprisingly, although wideband ambiguity functions have been quite extensively studied for a while, CRB for the delay-Doppler estimation of wideband signals has received less attention [18,19,22,28–30] leading to lack of a general compact closed-form CRB expression. Indeed, [18,19] derive CRB expressions in active [18] and passive system [19] for a wideband signal with known amplitude and phase. Since, in many applications, it is unrealistic to assume a known complex amplitude, several CRB expressions for the joint estimation of delay-Doppler and complex amplitude [28,29] or phase-amplitude [22,30] have been proposed. However, all of these expressions have been derived under unnecessary restrictive assumptions on the signal, in particular if the signal is assumed to be band-limited, leading to unnecessary restrictive CRB expressions. Moreover, none of the existing CRBs [18,19,22,28–30] provide closed-form expressions for the amplitude and phase, which may be of great interest in applications like GNSS or GNSS-R where the phase estimation performance drives the performance of subsequent estimation techniques, such as GNSS carrier phase-based precise positioning [40] or phase-based GNSS-R [41,42]. Thus, the contributions of this article are:

- The first contribution is a general compact closed-form CRB expression for the delay-Doppler estimation of a generic band-limited signal which is only supposed to have a finite number on non-zero samples, thus encompassing all existing CRB expressions.
- A second contribution is the introduction of a general compact closed-form CRB expression for the amplitude and phase.
- The compact CRBs obtained are expressed in terms of the baseband signal samples, making it especially easy to use whatever the baseband signal considered. This allows to exploit such expressions in a plethora of remote sensing applications.
- The validity of the new CRB expressions is assessed in the context of GNSS, both using synthetic and real data.

Notice that these results encompass the preliminary results for the delay-Doppler estimation assuming a narrowband signal recently derived in [32]. In comparison with the literature, including [32], a certain number of new terms appear in the proposed CRB due to the Doppler effect on the baseband signal which can not be guessed from existing results. For instance, for a real signal, the estimation of both parameters is not decoupled any longer.

Notation

Italic indicates a scalar quantity, as in a; lower case boldface indicates a column vector quantity, as in $\mathbf{a}$; upper case boldface indicates a matrix quantity, as in $\mathbf{A}$. The matrix/vector transpose is indicated by a superscript $(\cdot)^\top$ as in $\mathbf{A}^\top$, and the transpose conjugate $(\cdot)^H$ as in $\mathbf{A}^H$.

2. Signal Model

We consider the transmission of a band-limited (bandwidth B) signal $s(t)$ over a carrier frequency f_c ($\lambda_c = c/f_c$) from a transmitter T, at position $\mathbf{p}_T(t) = \mathbf{p}_T + \mathbf{v}_T t$, to a receiver R, at position $\mathbf{p}_R(t) = \mathbf{p}_R + \mathbf{v}_R t$ (uniform linear motions). The band-limited signal can be expressed in time/frequency (to be exploited for the bound derivation) as

$$s(t) = \sum_{n=N_1}^{N_2} s\left(\frac{n}{F_s}\right) \operatorname{sinc}\left(\pi F_s\left(t - \frac{n}{F_s}\right)\right), \tag{1}$$

$$s(f) = \left(\frac{1}{F_s}\sum_{n=N_1}^{N_2} s\left(\frac{n}{F_s}\right) e^{-j2\pi n\frac{f}{F_s}}\right) 1_{\left[-\frac{B}{2},\frac{B}{2}\right]}(f), \tag{2}$$

where $F_s \geq B$, and $N_1, N_2 \in \mathbb{Z}$, $N_1 \leq N_2$. The complex analytic signal at the output of the receiver's antenna can be written as

$$x_A(t) = \alpha_A s_A(t) + n_A(t), \tag{3}$$

with $n_A(t)$ a zero-mean white complex Gaussian noise, and where the gain α_A depends on the transmitted signal power, the transmitter/receiver antenna gains and polarization vectors, and the radial distance between T and R. If this distance, $\mathbf{p}_{TR}(t)$, can be approximated by a first order distance-velocity model [2,3,7,39],

$$\begin{aligned} &\|\mathbf{p}_{TR}(t)\| \triangleq \|\mathbf{p}_R(t) - \mathbf{p}_T(t - \tau(t))\| = c\tau(t) \simeq d + vt, \\ &\tau(t) \simeq \tau + bt, \quad \tau = \frac{d}{c},\ b = \frac{v}{c}, \quad c \simeq 3 \cdot 10^8\ m/s, \end{aligned} \tag{4}$$

so-called relative uniform radial movement, and characterized by a time-delay (τ) due to the propagation path and dilation ($1 - b$) induced by the Doppler effect. In this case [7,43],

$$s_A(t) = s((1-b)(t-\tau))\, e^{j2\pi f_c(1-b)t} e^{-j2\pi f_c \tau}. \tag{5}$$

Notice that the static signal model case in [44] is obtained with $b = 0$ ($\tau(t) \simeq \tau$), and the standard narrow-band signal model [2,3,7,20,29,31,32] is obtained by approximating $s((1-b)(t-\tau)) \simeq s(t-\tau)$. We can express the baseband output of the receiver's Hilbert filter as

$$x(t) = \alpha s(t; \boldsymbol{\eta})\, e^{-j\omega_c b(t-\tau)} + n(t), \tag{6}$$

where $\omega_c = 2\pi f_c$, $s(t;\boldsymbol{\eta}) = s((1-b)(t-\tau))$, $\boldsymbol{\eta} = [\tau, b]^\top$ and the complex gain $\alpha = \alpha_A e^{-j2\pi f_c(1+b)\tau}$. If F_s is the Hilbert filter bandwidth, then $n(t)$ is a complex white Gaussian noise within the bandwidth F_s with unknown variance σ_n^2. In addition, we have the following Nyquist–Shannon sampling condition: $f \in \left[-\frac{F_s}{2}, \frac{F_s}{2}\right]$ with $\frac{F_s}{2} \geq \max_b \left\{\frac{B}{2}(1-b)\right\}$. Both propagation time-delay and Doppler effect dilation are made apparent in

$$s(t;\boldsymbol{\eta}) = s((1-b)(t-\tau)) = s((1-b)u)|_{t-\tau} \tag{7}$$

$$\uparrow\downarrow$$

$$s(f;\boldsymbol{\eta}) = \frac{1}{1-b} s\left(\frac{f}{1-b}\right) e^{-j2\pi f\tau} \tag{8}$$

The discrete vector signal model is build from $N' = N_2' - N_1' + 1$ ($N_1' \ll N_1$, $N_2' \gg N_2$) samples at $T_s = 1/F_s$, meaning that the signal amplitude is assumed to be negligible outside the essential duration $\left[N_1' T_s, N_2' T_s\right]$,

$$\begin{aligned} \mathbf{x} &= \alpha \mathbf{a}(\boldsymbol{\eta}) + \mathbf{n}, \\ \mathbf{x} &= \left(x\left(N_1' T_s\right), \ldots, x\left(N_2' T_s\right)\right)^\top, \\ \mathbf{n} &= \left(n\left(N_1' T_s\right), \ldots, n\left(N_2' T_s\right)\right)^\top, \\ \mathbf{s}(\boldsymbol{\eta}) &= \left(s\left(N_1' T_s; \boldsymbol{\eta}\right), \ldots, s\left(N_2' T_s; \boldsymbol{\eta}\right)\right)^\top, \\ \mathbf{a}(\boldsymbol{\eta}) &= \left((\mathbf{s}(\boldsymbol{\eta}))_1 e^{-j\omega_c b\left(N_1' T_s - \tau\right)}, \ldots, (\mathbf{s}(\boldsymbol{\eta}))_{N'} e^{-j\omega_c b\left(N_2' T_s - \tau\right)}\right)^\top, \end{aligned} \tag{9}$$

where $\mathbf{n} \sim \mathcal{CN}\left(\mathbf{0}, \sigma_n^2 \mathbf{I}_{N'}\right)$. Since the transmitter/receiver antenna gains and polarization vectors are in general unknown to a certain extent, α is assumed to be an unknown complex parameter [4,8,9,35,43]. Then, the unknown deterministic parameters [36] can be gathered in vector $\underline{\epsilon}^\top = [\sigma_n^2, \alpha, \alpha^*, \boldsymbol{\eta}^\top]$, where α^* is the complex conjugate of α. Note that the same signal model (9) can be obtained if instead of line-of-sight transmission, one considers transmission via diffraction (scatterer), reflexion (reflector) or combination of the three (multipaths) [8,43].

3. Maximum Likelihood and Ambiguity Function

Considering the signal model (9), the delay-Doppler MLE is defined as (Let $S = span(\mathbf{A})$, with $\mathbf{A}$ a matrix, be the linear span of the set of its column vectors, $S^\perp$ the orthogonal complement of the subspace S, $\boldsymbol{\Pi}_{\mathbf{A}} = \mathbf{A}\left(\mathbf{A}^H \mathbf{A}\right) \mathbf{A}^H$ the orthogonal projection over S, and $\boldsymbol{\Pi}_{\mathbf{A}}^\perp = \mathbf{I} - \boldsymbol{\Pi}_{\mathbf{A}}$) [35]

$$\widehat{\boldsymbol{\eta}} = \arg\min_{\boldsymbol{\eta}} \left\{\mathbf{x}^H \boldsymbol{\Pi}_{\mathbf{a}(\boldsymbol{\eta})}^\perp \mathbf{x}\right\} = \arg\max_{\boldsymbol{\eta}} \left\{\frac{\left|\mathbf{a}(\boldsymbol{\eta})^H \mathbf{x}\right|^2}{\mathbf{a}(\boldsymbol{\eta})^H \mathbf{a}(\boldsymbol{\eta})}\right\} = \arg\max_{(b,\tau)} \left\{\frac{\left|\int_{-\infty}^{+\infty} s(t;\boldsymbol{\eta})^* e^{j\omega_c b(t-\tau)} x(t) dt\right|^2}{\frac{1}{(1-b)} \int_{-\infty}^{+\infty} |s(t)|^2 dt}\right\}, \tag{10}$$

which is instrumental to validate a CRB expression because such estimator is known to be asymptotically efficient (e.g., in the high SNR regime) for the conditional signal model of interest [16,17]. Another interesting expression is the maximum SNR at the output of the MLE matched filter

$$\mathrm{SNR}_{\mathrm{out}} = \frac{\left|\int_{-\infty}^{+\infty} s(t;\boldsymbol{\eta})^* \alpha s(t;\boldsymbol{\eta}) dt\right|^2}{E\left[\left|\int_{-\infty}^{+\infty} s(t;\boldsymbol{\eta})^* n(t) dt\right|^2\right]} = \frac{|\alpha|^2}{\left(\frac{\sigma_{\tilde{n}}^2}{F_s}\right)(1-b)} \int_{-\infty}^{+\infty} |s(t)|^2 dt = \frac{|\alpha|^2 \mathbb{E}}{\left(\frac{\sigma_{\tilde{\mathbf{n}}}^2}{F_s}\right)(1-b)}, \tag{11}$$

with $\mathbb{E} = \int_{-\infty}^{+\infty} |s(t)|^2 dt$ the energy of the signal. The corresponding ambiguity function is given by [2,3,7,43]

$$\Xi\left(\boldsymbol{\eta}'; \boldsymbol{\eta}\right) = \frac{1}{N'} \left(\mathbf{a}(\boldsymbol{\eta}) \alpha\right)^H \boldsymbol{\Pi}_{\mathbf{a}(\boldsymbol{\eta}')} \left(\mathbf{a}(\boldsymbol{\eta}) \alpha\right) = \frac{|\alpha|^2}{N'} \|\mathbf{a}(\boldsymbol{\eta})\|^2 \left|\frac{\mathbf{a}(\boldsymbol{\eta})^H \mathbf{a}(\boldsymbol{\eta}')}{\|\mathbf{a}(\boldsymbol{\eta})\| \|\mathbf{a}(\boldsymbol{\eta}')\|}\right|^2, \tag{12}$$

and if we define the following function

$$\boldsymbol{\Phi}(\boldsymbol{\eta}) = \frac{\partial \mathbf{a}(\boldsymbol{\eta})}{\partial \boldsymbol{\eta}^T}^H \boldsymbol{\Pi}_{\mathbf{a}(\boldsymbol{\eta})}^\perp \frac{\partial \mathbf{a}(\boldsymbol{\eta})}{\partial \boldsymbol{\eta}^T}, \tag{13}$$

it can be approximated by its 2nd order Taylor expansion as [7] (Chapter 3.9.4)

$$\Xi\left(\boldsymbol{\eta}+d\boldsymbol{\eta};\boldsymbol{\eta}\right)\simeq\frac{|\alpha|^2}{N'}\left\|\mathbf{a}\left(\boldsymbol{\eta}\right)\right\|^2\left(1-\frac{1}{2}d\boldsymbol{\eta}^T\left(\frac{2\Re\left\{\boldsymbol{\Phi}\left(\boldsymbol{\eta}\right)\right\}}{\left\|\mathbf{a}\left(\boldsymbol{\eta}\right)\right\|^2}\right)d\boldsymbol{\eta}\right), \tag{14}$$

where the second term which depends on $\Phi\left(\boldsymbol{\eta}\right)$ is directly related to the CRB (see (15)–(24)). Since the true and approximated ambiguity function must coincide around the maximum, this is also helpful to validate the CRB expression.

4. New Compact CRB for Delay, Doppler Stretch and Phase Estimation with a Band-limited Signal

The main goal of this contribution is to obtain a new compact analytic form of the CRB for the signal model (9), where both time-delay τ and time-delay drift b, also known as the Doppler effect leading to time compression or expansion, are to be estimated (i.e., $\tau(t)\approx\tau+bt$).

4.1. Background on CRB for the Single Source CSM

The CRB of $\boldsymbol{\eta}$ for a Gaussian conditional observation model (9) has been known for ages [34] and is given by [6,34–36]

$$\mathbf{CRB}_{\boldsymbol{\eta}}=\frac{\sigma_n^2}{2\left|\alpha\right|^2}\Re\left\{\boldsymbol{\Phi}\left(\boldsymbol{\eta}\right)\right\}^{-1},\ \boldsymbol{\Phi}\left(\boldsymbol{\eta}\right)\triangleq(13). \tag{15}$$

Thus, there is no point in recomputing the global Fisher Information Matrix (FIM) [36]

$$\mathbf{F}_{\underline{\boldsymbol{\epsilon}}}=E\left[\frac{\partial\ln p\left(\mathbf{x};\underline{\boldsymbol{\epsilon}}\right)}{\partial\underline{\boldsymbol{\epsilon}}}\left(\frac{\partial\ln p\left(\mathbf{x};\underline{\boldsymbol{\epsilon}}\right)}{\partial\underline{\boldsymbol{\epsilon}}}\right)^H\right]=-E\left[\frac{\partial^2\ln p\left(\mathbf{x};\underline{\boldsymbol{\epsilon}}\right)}{\partial\underline{\boldsymbol{\epsilon}}\partial\underline{\boldsymbol{\epsilon}}^H}\right], \tag{16}$$

to extract $\mathbf{CRB}_{\boldsymbol{\eta}}$ (15) as proposed previously in [22,28–30] (even in the multiple sources case as in [29], since a multiple sources version of (15) exists as well [6,34–36]) which may lead to errors in its derivation. Interestingly enough, if we reparameterize the complex amplitude α as $\alpha=\rho e^{j\varphi}$ where ρ denotes the amplitude (modulus) and φ the phase, then (9) becomes

$$\mathbf{x}=\rho e^{j\varphi}\mathbf{a}\left(\boldsymbol{\eta}\right)+\mathbf{n}, \tag{17}$$

and the unknown deterministic parameter vector $\underline{\boldsymbol{\epsilon}}$ becomes $\boldsymbol{\epsilon}^\top=[\sigma_n^2,\rho,\varphi,\boldsymbol{\eta}^\top]$. Under this equivalent parameterization of the conditional observation model, the compact $\mathbf{CRB}_{\boldsymbol{\eta}}$ (15) can be complemented in order to include amplitude and phase parameters [32], which leads to

$$CRB_\rho=\frac{\sigma_n^2}{2\left\|\mathbf{a}\left(\boldsymbol{\eta}\right)\right\|^2}+\rho^2\frac{\mathrm{Re}\left\{\mathbf{a}^H\left(\boldsymbol{\eta}\right)\frac{\partial\mathbf{a}(\boldsymbol{\eta})}{\partial\boldsymbol{\eta}^\top}\right\}\mathbf{CRB}_{\boldsymbol{\eta}}\,\mathrm{Re}\left\{\mathbf{a}^H\left(\boldsymbol{\eta}\right)\frac{\partial\mathbf{a}(\boldsymbol{\eta})}{\partial\boldsymbol{\eta}^\top}\right\}^\top}{\left\|\mathbf{a}\left(\boldsymbol{\eta}\right)\right\|^4}, \tag{18}$$

$$\mathbf{CRB}_{\boldsymbol{\theta}}=\begin{bmatrix}CRB_\varphi & \mathbf{CRB}_{\boldsymbol{\eta},\varphi}^\top\\ \mathbf{CRB}_{\boldsymbol{\eta},\varphi} & \mathbf{CRB}_{\boldsymbol{\eta}}\end{bmatrix},\ \boldsymbol{\theta}^\top=\left(\varphi,\boldsymbol{\eta}^\top\right), \tag{19}$$

where $\mathbf{CRB}_{\boldsymbol{\eta}}$ is given by (15) and

$$CRB_\varphi=\frac{\sigma_n^2}{2\rho^2}\frac{1}{\left\|\mathbf{a}\left(\boldsymbol{\eta}\right)\right\|^2}+\frac{\mathrm{Im}\left\{\mathbf{a}^H\left(\boldsymbol{\eta}\right)\frac{\partial\mathbf{a}(\boldsymbol{\eta})}{\partial\boldsymbol{\eta}^\top}\right\}\mathbf{CRB}_{\boldsymbol{\eta}}\,\mathrm{Im}\left\{\mathbf{a}^H\left(\boldsymbol{\eta}\right)\frac{\partial\mathbf{a}(\boldsymbol{\eta})}{\partial\boldsymbol{\eta}^\top}\right\}^\top}{\left\|\mathbf{a}\left(\boldsymbol{\eta}\right)\right\|^4}, \tag{20}$$

$$\mathbf{CRB}_{\boldsymbol{\eta},\varphi}=-\mathbf{CRB}_{\boldsymbol{\eta}}\frac{\mathrm{Im}\left\{\mathbf{a}^H\left(\boldsymbol{\eta}\right)\frac{\partial\mathbf{a}(\boldsymbol{\eta})}{\partial\boldsymbol{\eta}^\top}\right\}^\top}{\left\|\mathbf{a}\left(\boldsymbol{\eta}\right)\right\|^2}. \tag{21}$$

Last, since $\mathrm{SNR}_{\mathrm{out}} = \rho^2 / \left(\sigma_{\mathbf{n}}^2 (1-b)\right) \mathbb{E}F_s$ (11), it may be worth remembering that [6,35]

$$CRB_{\sigma_n^2} = \frac{1}{N'} \left(\sigma_n^2\right)^2, \tag{22}$$

which allows to compute $CRB_{\mathrm{SNR}_{\mathrm{out}}}$, of interest in some applications.

For the sake of completeness, under the reparametrized conditional observation model (17), the amplitude ρ and phase φ MLEs are given by [35]

$$\widehat{\rho} = |\widehat{\alpha}|, \quad \widehat{\varphi} = \arg\{\widehat{\alpha}\}, \quad \widehat{\alpha} = \frac{\mathbf{a}(\boldsymbol{\eta})^H \mathbf{x}}{\mathbf{a}(\boldsymbol{\eta})^H \mathbf{a}(\boldsymbol{\eta})} = \frac{\int_{-\infty}^{+\infty} s(t;\boldsymbol{\eta})^* e^{j\omega_c b(t-\tau)} x(t)\, dt}{\frac{1}{(1-b)} \int_{-\infty}^{+\infty} |s(t)|^2 dt}, \tag{23}$$

where $\widehat{\alpha}$ is the MLE of the complex amplitude α.

4.2. A Preliminary Compact CRB for the Single Band-Limited Source CSM

Let $\beta = 1 - b$ and $s^{(1)}(t) = \frac{ds(t)}{dt}$. Thus, we look for the compact closed-form analytic expression,

$$\begin{aligned} \Re\{\boldsymbol{\Phi}(\boldsymbol{\eta})\} &= \begin{bmatrix} (\cdot)_{1,1} & (\cdot)_{1,2} \\ (\cdot)_{1,2} & (\cdot)_{2,2} \end{bmatrix} \\ &= \Re\left\{ \frac{\partial \mathbf{a}(\boldsymbol{\eta})}{\partial \boldsymbol{\eta}^\top}^H \frac{\partial \mathbf{a}(\boldsymbol{\eta})}{\partial \boldsymbol{\eta}^\top} \right\} - \Re\left\{ \frac{1}{\|\mathbf{a}(\boldsymbol{\eta})\|^2} \left(\mathbf{a}(\boldsymbol{\eta})^H \frac{\partial \mathbf{a}(\boldsymbol{\eta})}{\partial \boldsymbol{\eta}^\top} \right)^H \left(\mathbf{a}(\boldsymbol{\eta})^H \frac{\partial \mathbf{a}(\boldsymbol{\eta})}{\partial \boldsymbol{\eta}^\top} \right) \right\}, \end{aligned} \tag{24}$$

which after tedious calculus (details in Appendix A) is given by

$$\begin{aligned} (\cdot)_{1,1} &= F_s \beta^2 \left(W_{3,3} - \tfrac{|w_3|^2}{w_1} \right), \\ (\cdot)_{1,2} &= F_s \beta \left(\omega_c \Im\left\{ w_4 - \tfrac{w_3 w_2}{w_1} \right\} - \tfrac{1}{w_1} \Re\{w_3 w_4^*\} + W_{4,3} \right), \\ (\cdot)_{2,2} &= F_s \left(\omega_c^2 \left(W_{2,2} - \tfrac{w_2^2}{w_1} \right) + 2\omega_c \Im\left\{ W_{4,2} - \tfrac{w_2 w_4}{w_1} \right\} + W_{4,4} - \tfrac{|w_4|^2}{w_1} \right), \end{aligned} \tag{25}$$

where

$$\mathbf{a}^H(\boldsymbol{\eta}) \frac{\partial \mathbf{a}(\boldsymbol{\eta})}{\partial \boldsymbol{\eta}^T} = F_s \begin{pmatrix} j\omega_c (1-\beta) w_1 - \beta w_3 \\ -j\omega_c w_2 - w_4 \end{pmatrix}^\top, \tag{26}$$

and the terms w_1, w_2, w_3, w_4, $W_{2,2}$, $W_{3,3}$, $W_{4,2}$, $W_{4,3}$, $W_{4,4}$ are computed as

$$
\begin{aligned}
w_1 &= \frac{1}{\beta}\int_{-\infty}^{+\infty} |s(t)|^2\,dt,\ w_2 = \frac{1}{\beta^2}\int_{-\infty}^{+\infty} t\,|s(t)|^2\,dt,\\
w_3 &= \frac{1}{\beta}\int_{-\infty}^{+\infty} s^{(1)}(t)\,s(t)^*\,dt,\ w_4 = \frac{1}{\beta^2}\int_{-\infty}^{+\infty} ts^{(1)}(t)\,s(t)^*\,dt,\\
W_{2,2} &= \frac{1}{\beta^3}\int_{-\infty}^{+\infty} t^2\,|s(t)|^2\,dt,\ W_{3,3} = \frac{1}{\beta}\int_{-\infty}^{+\infty} \left|s^{(1)}(t)\right|^2\,dt,\\
W_{4,2} &= \frac{1}{\beta^3}\int_{-\infty}^{+\infty} t^2 s^{(1)}(t)\,s(t)^*\,dt,\ W_{4,3} = \frac{1}{\beta^2}\int_{-\infty}^{+\infty} t\left|s^{(1)}(t)\right|^2\,dt,\\
W_{4,4} &= \frac{1}{\beta^3}\int_{-\infty}^{+\infty} t^2\left|s^{(1)}(t)\right|^2\,dt.
\end{aligned}
\tag{27}
$$

4.3. Comparison with Existing Literature

In the existing literature [18,19,22,28–30], whenever the signal amplitude ρ and phase φ are known, the observation model does not explicitly take into account a complex envelope modulated by a carrier frequency f_c as in (6), (9), (17), but is simply [18] ((1.1), (1.8)), [19] ((2), (11)), [22] (1), [28] (4), [29] ((2), (5)), [30] (1),

$$
x(t) = \alpha s(t;\boldsymbol{\eta}) + n(t),
\tag{28}
$$

where $s(t;\boldsymbol{\eta})$ is a band-limited signal (since the noise $n(t)$ is always assumed to be band-limited, with a bandwidth being larger than (or equal to) the signal bandwidth). Thus (28) amounts to set $f_c = 0$ in both observation models (6), (9), (17) and CRB terms (25), (26), leading to

$$
\mathbf{CRB}_{\boldsymbol{\eta}} = \frac{\sigma_n^2}{2\rho^2}\boldsymbol{\Lambda}^{-1},\quad
\begin{aligned}
\Lambda_{1,1} &= F_s\beta^2\left(W_{3,3} - \tfrac{|w_3|^2}{w_1}\right),\\
\Lambda_{1,2} &= F_s\beta\left(W_{4,3} - \tfrac{\Re\{w_3 w_4^*\}}{w_1}\right),\\
\Lambda_{2,1} &= \Lambda_{1,2},\\
\Lambda_{2,2} &= F_s\left(W_{4,4} - \tfrac{|w_4|^2}{w_1}\right).
\end{aligned}
\tag{29}
$$

If we consider the existing literature where the signal amplitude ρ and phase φ are unknown [22,28,30], it takes into account that $\Re\{w_3\} = 0$ (true for any $s(t)$, see next Section) but also that $\Re\{w_4\} = 0$ which is an unnecessary restriction not satisfied for most of real-valued signals (see next Section), leading to [22] (14), [28] (10), [30] (Section IV) (with a few typos [22] ((12e–12g)), [30] (13)),

$$
\mathbf{CRB}_{\boldsymbol{\eta}} = \frac{\sigma_n^2}{2\rho^2}\boldsymbol{\Lambda}^{-1},\quad
\begin{aligned}
\Lambda_{1,1} &= F_s\beta^2\left(W_{3,3} - \tfrac{\mathrm{Im}\{w_3^*\}^2}{w_1}\right),\\
\Lambda_{1,2} &= F_s\beta\left(W_{4,3} - \tfrac{\mathrm{Im}\{w_3^*\}\,\mathrm{Im}\{w_4^*\}}{w_1}\right),\\
\Lambda_{2,1} &= \Lambda_{1,2},\\
\Lambda_{2,2} &= F_s\left(W_{4,4} - \tfrac{\mathrm{Im}\{w_4^*\}^2}{w_1}\right),
\end{aligned}
\tag{30}
$$

which is (29) under $\Re\{w_3\} = \Re\{w_4\} = 0$. Last, if we consider the existing literature where the signal amplitude ρ is unknown but the phase φ is known [29], the single point target case detailed for a real-valued α reads,

$$\mathbf{CRB}_{\boldsymbol{\eta}} = \frac{\sigma_n^2}{2\rho^2}\boldsymbol{\Lambda}^{-1}, \begin{array}{l} \Lambda_{1,1} = F_s\beta^2 W_{3,3}, \\ \Lambda_{1,2} = F_s\beta W_{4,3}, \\ \Lambda_{2,1} = \Lambda_{1,2}, \\ \Lambda_{2,2} = F_s\left(W_{4,4} - \frac{\Re\{w_4\}^2}{w_1}\right), \end{array} \tag{31}$$

where assumption ([18], (1.12)) is taken into account leading to ([18], (1.15)) $\Re\{w_4\} = -w_1/(2\beta)$ and $\Re\{w_4\}^2/w_1 = w_1/\left(4\beta^2\right)$. Note that assumption ([18], (1.12)) is not satisfied by a great number of band-limited signals (for instance if $s(t) = s(0)\mathrm{sinc}(\pi F_s t)$). Additionally note that neither CRB_ρ (18) nor $\mathbf{CRB}_{\boldsymbol{\theta}}$ (19) have been introduced in the existing literature dealing with Doppler stretch. Thus, the proposed approach where the only assumption is to consider a band-limited signal having a finite number on non-zero samples (to ensure finiteness of all the integrals considered (27) as detailed in the next Section), and an explicit carrier frequency modulation, offer far more general (or new) CRB expressions than the existing ones (from which w_2, $W_{2,2}$, $W_{4,2}$ can not be guessed).

4.4. A Versatile Compact CRB for Delay, Doppler Stretch and Phase Estimation with a Band-Limited Signal

Even if deriving the most general form of the CRBs (15), (18), (19), (25), (26) and (27) for a given observation model and a given class of signals is of theoretical importance, making it easy to apply for a large subset of the class, and ideally to the whole class, is also a challenging goal of great interest both from a practical and a theoretical point of view. Actually, such easy to use and versatile expressions can be introduced by exploiting the properties of a band-limited signal (1). Indeed, in that case, the terms $w_1, w_2, \ldots, W_{4,3}, W_{4,4}$ (27) can also be expressed as (details in Appendix B)

$$\begin{aligned} &w_1 = \frac{\mathbf{s}^H\mathbf{s}}{\beta F_s},\ w_2 = \frac{\mathbf{s}^H\mathbf{D}\mathbf{s}}{\beta^2 F_s^2},\ w_3 = \frac{\mathbf{s}^H\boldsymbol{\Lambda}\mathbf{s}}{\beta}, w_4 = \frac{\mathbf{s}^H\mathbf{D}\boldsymbol{\Lambda}\mathbf{s}}{\beta^2 F_s},\ W_{2,2} = \frac{\mathbf{s}^H\mathbf{D}^2\mathbf{s}}{\beta^3 F_s^3},\ W_{3,3} = \frac{F_s\mathbf{s}^H\mathbf{V}\mathbf{s}}{\beta}, \\ &W_{4,2} = \frac{1}{\beta^3 F_s^2}\left(\mathbf{s}^H\mathbf{D}\boldsymbol{\Lambda}\mathbf{D}\mathbf{s} - \mathbf{s}^H\mathbf{D}\mathbf{s}\right), W_{4,3} = \frac{1}{\beta^2}\left(\mathbf{s}^H\boldsymbol{\Lambda}\mathbf{s} + \mathbf{s}^H\mathbf{V}\mathbf{D}\mathbf{s}\right), \\ &W_{4,4} = \frac{1}{\beta^3 F_s}\left(\mathbf{s}^H\mathbf{s} + \mathbf{s}^H\mathbf{D}\mathbf{V}\mathbf{D}\mathbf{s} - 2\Re\left\{\mathbf{s}^H\boldsymbol{\Lambda}\mathbf{D}\mathbf{s}\right\}\right), \end{aligned} \tag{32}$$

with $\mathbf{D}$, $\boldsymbol{\Lambda}$ and $\mathbf{V}$ defined as

$$\mathbf{D} = \mathrm{diag}\left([N_1,\ N_1+1, \ldots,\ N_2-1,\ N_2]\right), \tag{33}$$

$$(\mathbf{V})_{n,n'} = \begin{array}{|l} n' \neq n : (-1)^{|n-n'|}\frac{2}{(n-n')^2} \\ n' = n : \frac{\pi^2}{3} \end{array}, \tag{34}$$

$$(\boldsymbol{\Lambda})_{n,n'} = \begin{array}{|l} n' \neq n : \frac{(-1)^{|n-n'|}}{(n-n')} \\ n' = n : 0 \end{array}, \tag{35}$$

for $N_1 \leq n, n' \leq N_2$. Moreover, since $W_{3,3} > 0$ if $\mathbf{s} \neq \mathbf{0}$, then $\mathbf{V}$ is a symmetric positive definite real-valued matrix $\left(\mathbf{V}^T = \mathbf{V}, \mathbf{V} > \mathbf{0}\right)$; and $\boldsymbol{\Lambda}$ is an anti-symmetric real-valued matrix $\left(\boldsymbol{\Lambda}^T = -\boldsymbol{\Lambda}\right)$, which leads to $\Re\left\{\mathbf{s}^H\boldsymbol{\Lambda}\mathbf{s}\right\} = 0$ and $\Re\left\{\mathbf{s}^H\mathbf{D}\boldsymbol{\Lambda}\mathbf{D}\mathbf{s}\right\} = 0$. Finally, the terms in (25), (26) can be expressed as

$$
\begin{aligned}
(\cdot)_{1,1} &= F_s\beta\mathbf{s}^H\mathbf{s}\left(\frac{\mathbf{s}^H\mathbf{V}\mathbf{s}}{\mathbf{s}^H\mathbf{s}}-\left|\frac{\mathbf{s}^H\mathbf{\Lambda}\mathbf{s}}{\mathbf{s}^H\mathbf{s}}\right|^2\right)\\
(\cdot)_{1,2} &= \frac{\mathbf{s}^H\mathbf{s}}{\beta}\left(\frac{\omega_c}{F_s}\Im\left\{\frac{\mathbf{s}^H\mathbf{D}\mathbf{\Lambda}\mathbf{s}}{\mathbf{s}^H\mathbf{s}}-\frac{\mathbf{s}^H\mathbf{\Lambda}\mathbf{s}}{\mathbf{s}^H\mathbf{s}}\frac{\mathbf{s}^H\mathbf{D}\mathbf{s}}{\mathbf{s}^H\mathbf{s}}\right\}-\Re\left\{\frac{\mathbf{s}^H\mathbf{\Lambda}\mathbf{s}}{\mathbf{s}^H\mathbf{s}}\frac{\mathbf{s}^H\mathbf{\Lambda}\mathbf{D}\mathbf{s}}{\mathbf{s}^H\mathbf{s}}\right\}+\frac{\mathbf{s}^H\mathbf{\Lambda}\mathbf{s}}{\mathbf{s}^H\mathbf{s}}+\frac{\mathbf{s}^H\mathbf{V}\mathbf{D}\mathbf{s}}{\mathbf{s}^H\mathbf{s}}\right),\\
(\cdot)_{2,2} &= \frac{\mathbf{s}^H\mathbf{s}}{F_s\beta^3}\left(\begin{array}{l}\frac{\omega_c^2}{F_s^2}\left(\frac{\mathbf{s}^H\mathbf{D}^2\mathbf{s}}{\mathbf{s}^H\mathbf{s}}-\left(\frac{\mathbf{s}^H\mathbf{D}\mathbf{s}}{\mathbf{s}^H\mathbf{s}}\right)^2\right)+2+\frac{\mathbf{s}^H\mathbf{D}\mathbf{V}\mathbf{D}\mathbf{s}}{\mathbf{s}^H\mathbf{s}}-\left|1+\frac{\mathbf{s}^H\mathbf{\Lambda}\mathbf{D}\mathbf{s}}{\mathbf{s}^H\mathbf{s}}\right|^2\\ +2\frac{\omega_c}{F_s}\Im\left\{\frac{\mathbf{s}^H\mathbf{D}\mathbf{\Lambda}\mathbf{D}\mathbf{s}}{\mathbf{s}^H\mathbf{s}}-\frac{\mathbf{s}^H\mathbf{D}\mathbf{s}}{\mathbf{s}^H\mathbf{s}}\right\}-2\frac{\omega_c}{F_s}\Im\left\{\frac{\mathbf{s}^H\mathbf{D}\mathbf{s}}{\mathbf{s}^H\mathbf{s}}\frac{\mathbf{s}^H\mathbf{D}\mathbf{\Lambda}\mathbf{s}}{\mathbf{s}^H\mathbf{s}}\right\}\end{array}\right)
\end{aligned}
\tag{36}
$$

$$
\mathbf{a}(\boldsymbol{\eta})^H\frac{\partial\mathbf{a}(\boldsymbol{\eta})}{\partial\boldsymbol{\eta}^T}=F_s\mathbf{s}^H\mathbf{s}\left(\begin{array}{c}j\frac{\omega_c}{\beta F_s}(1-\beta)-\frac{\mathbf{s}^H\mathbf{\Lambda}\mathbf{s}}{\mathbf{s}^H\mathbf{s}}-j\frac{\omega_c}{\beta^2F_s^2}\frac{\mathbf{s}^H\mathbf{D}\mathbf{s}}{\mathbf{s}^H\mathbf{s}}-\frac{1}{\beta^2F_s}\frac{\mathbf{s}^H\mathbf{D}\mathbf{\Lambda}\mathbf{s}}{\mathbf{s}^H\mathbf{s}}\end{array}\right)^\top. \tag{37}
$$

From this result, it is straightforward to obtain compact closed-form CRB expressions for (15), (18), (19) (i.e., (24) is a 2×2 matrix) which depend only on the baseband signal samples and known matrices $\mathbf{D}$, $\mathbf{V}$ and $\mathbf{\Lambda}$ (33)–(35). These appealing closed-form CRBs which depend only on the samples' vector, can thus be used for any sensing application compliant with the CSM (6) in order to investigate its asymptotic theoretical performance, and possibly, to assess the threshold region by comparing simulated (or measured) MSE of MLEs with the CRBs values obtained.

In addition, if $s(t)$ is a real-valued signal, then $\Re\{\mathbf{s}^\top\mathbf{\Lambda}\mathbf{s}\}=\Re\{\mathbf{s}^\top\mathbf{D}\mathbf{\Lambda}\mathbf{D}\mathbf{s}\}=0$ and (36–37) simplify to

$$
\begin{aligned}
(\cdot)_{1,1} &= F_s\beta\mathbf{s}^\top\mathbf{s}\frac{\mathbf{s}^\top\mathbf{V}\mathbf{s}}{\mathbf{s}^\top\mathbf{s}},\\
(\cdot)_{1,2} &= \frac{\mathbf{s}^\top\mathbf{s}}{\beta}\frac{\mathbf{s}^\top\mathbf{V}\mathbf{D}\mathbf{s}}{\mathbf{s}^\top\mathbf{s}},\\
(\cdot)_{2,2} &= \frac{\mathbf{s}^\top\mathbf{s}}{F_s\beta^3}\left(\frac{\omega_c^2}{F_s^2}\left(\frac{\mathbf{s}^\top\mathbf{D}^2\mathbf{s}}{\mathbf{s}^\top\mathbf{s}}-\left(\frac{\mathbf{s}^\top\mathbf{D}\mathbf{s}}{\mathbf{s}^\top\mathbf{s}}\right)^2\right)+2+\frac{\mathbf{s}^\top\mathbf{D}\mathbf{V}\mathbf{D}\mathbf{s}}{\mathbf{s}^\top\mathbf{s}}-\left(1+\frac{\mathbf{s}^\top\mathbf{D}\mathbf{\Lambda}\mathbf{s}}{\mathbf{s}^\top\mathbf{s}}\right)^2\right),
\end{aligned}
\tag{38}
$$

$$
\mathbf{a}(\boldsymbol{\eta})^H\frac{\partial\mathbf{a}(\boldsymbol{\eta})}{\partial\boldsymbol{\eta}^T}=F_s\mathbf{s}^\top\mathbf{s}\left(j\frac{\omega_c}{\beta F_s}(1-\beta)-j\frac{\omega_c}{\beta^2F_s^2}\frac{\mathbf{s}^\top\mathbf{D}\mathbf{s}}{\mathbf{s}^\top\mathbf{s}}-\frac{1}{\beta^2F_s}\frac{\mathbf{s}^\top\mathbf{D}\mathbf{\Lambda}\mathbf{s}}{\mathbf{s}^\top\mathbf{s}}\right)^\top. \tag{39}
$$

4.5. Standard Narrowband Signal Model

A simplified narrowband signal model is analyzed in [20,32], where the Doppler effect on the baseband signal $s(t)$ is not considered. In this case, $a(t;\boldsymbol{\eta})$ is written as

$$
s\left((1-b)(t-\tau)\right)e^{-j\omega_c bt}\simeq s(t-\tau)e^{-j\omega_c bt}. \tag{40}
$$

Under this hypothesis, (36) and (37) become [20,32]

$$
\begin{aligned}
(.)_{1,1} &= F_s\mathbf{s}^H\mathbf{s}\left(\frac{\mathbf{s}^H\mathbf{V}\mathbf{s}}{\mathbf{s}^H\mathbf{s}}-\left|\frac{\mathbf{s}^H\mathbf{\Lambda}\mathbf{s}}{\mathbf{s}^H\mathbf{s}}\right|^2\right)\\
(.)_{1,2} &= \frac{\mathbf{s}^H\mathbf{c}}{F_s}\left(\omega_c\Im\left\{\frac{\mathbf{s}^H\mathbf{D}\mathbf{\Lambda}\mathbf{s}}{\mathbf{s}^H\mathbf{s}}-\frac{\mathbf{s}^H\mathbf{\Lambda}\mathbf{s}}{\mathbf{s}^H\mathbf{s}}\frac{\mathbf{s}^H\mathbf{D}\mathbf{s}}{\mathbf{s}^H\mathbf{s}}\right\}\right),\\
(.)_{2,2} &= \frac{\mathbf{s}^H\mathbf{s}}{F_s}\frac{\omega_c^2}{F_s^2}\left(\frac{\mathbf{s}^H\mathbf{D}^2\mathbf{s}}{\mathbf{s}^H\mathbf{s}}-\left(\frac{\mathbf{s}^H\mathbf{D}\mathbf{s}}{\mathbf{s}^H\mathbf{s}}\right)^2\right)
\end{aligned}
\tag{41}
$$

and [32]

$$
\mathbf{a}(\boldsymbol{\eta})^H\frac{\partial\mathbf{a}(\boldsymbol{\eta})}{\partial\boldsymbol{\eta}^T}=F_s\mathbf{s}^H\mathbf{s}\left(\begin{array}{c}j\frac{\omega_c}{\beta F_s}(1-\beta)-\frac{\mathbf{s}^H\mathbf{\Lambda}\mathbf{s}}{\mathbf{s}^H\mathbf{s}}\\ -j\frac{\omega_c}{\beta^2F_s^2}\frac{\mathbf{s}^H\mathbf{D}\mathbf{s}}{\mathbf{s}^H\mathbf{s}}\end{array}\right)^\top. \tag{42}
$$

Then, if $s(t)$ is a real signal, (41), (42), reduce to

$$\begin{array}{l}(.)_{1,1} = F_s \mathbf{s}^\top \mathbf{s} \frac{\mathbf{s}^\top \mathbf{V} \mathbf{s}}{\mathbf{s}^\top \mathbf{s}} \\ (.)_{1,2} = 0 \\ (.)_{2,2} = \frac{\mathbf{s}^\top \mathbf{s}}{F_s} \frac{\omega_c^2}{F_s^2} \left(\frac{\mathbf{s}^\top \mathbf{D}^2 \mathbf{s}}{\mathbf{s}^\top \mathbf{s}} - \left(\frac{\mathbf{s}^\top \mathbf{D} \mathbf{s}}{\mathbf{s}^\top \mathbf{s}} \right)^2 \right) \end{array}, \tag{43}$$

and

$$\mathbf{a}(\boldsymbol{\eta})^H \frac{\partial \mathbf{a}(\boldsymbol{\eta})}{\partial \boldsymbol{\eta}^T} = j F_s \mathbf{s}^\top \mathbf{s} \frac{\omega_c}{\beta F_s} \begin{pmatrix} 1-\beta \\ -\frac{1}{\beta F_s} \frac{\mathbf{s}^\top \mathbf{D} \mathbf{s}}{\mathbf{s}^\top \mathbf{s}} \end{pmatrix}^\top, \tag{44}$$

Notice that $\Re\{\boldsymbol{\Phi}(\boldsymbol{\eta})\}_{2,2}$ has become invariant by time translation because it comes only from the term $e^{-j\omega_c b(t-\tau)}$.

4.6. Further Insights and Outlooks

The versatility of the proposed CRB expressions is a key feature that can be easily emphasized by the following (non exhaustive) list of examples of use. For instance, one important outcome offered by the new CRB expressions based on (36) and (37) is to allow a quantifiable assessment of the impact of a bandwidth increase on the CRB values, and also on the coupling between the delay and Doppler effect. Firstly, we can see that for real narrowband signals, the estimation of both parameters is decoupled because the cross terms are null (43), which is no longer the case when the bandwidth increases (38). Secondly, one can notice that an increase of bandwidth has mainly an impact on the Doppler estimation and a marginal impact on the delay estimation by coupling, since

$$\begin{array}{rcl}(.)_{1,1}^{WB} & = & F_s \beta \mathbf{s}^H \mathbf{s} \left(\frac{\mathbf{s}^H \mathbf{V} \mathbf{s}}{\mathbf{s}^H \mathbf{s}} - \left| \frac{\mathbf{s}^H \boldsymbol{\Lambda} \mathbf{s}}{\mathbf{s}^H \mathbf{s}} \right|^2 \right) = (.)_{1,1}^{NB} \\ (.)_{2,2}^{WB} & \simeq & (.)_{2,2}^{NB} + \frac{\mathbf{s}^H \mathbf{s}}{F_s} \begin{pmatrix} 2 + \frac{\mathbf{s}^H \mathbf{D} \mathbf{V} \mathbf{D} \mathbf{s}}{\mathbf{s}^H \mathbf{s}} - \left| 1 + \frac{\mathbf{s}^H \boldsymbol{\Lambda} \mathbf{D} \mathbf{s}}{\mathbf{s}^H \mathbf{s}} \right|^2 \\ 2\frac{\omega_c}{F_s} \Im \left\{ \frac{\mathbf{s}^H \mathbf{D} \boldsymbol{\Lambda} \mathbf{D} \mathbf{s}}{\mathbf{s}^H \mathbf{s}} - \frac{\mathbf{s}^H \mathbf{D} \mathbf{s}}{\mathbf{s}^H \mathbf{s}} \right\} - 2\frac{\omega_c}{F_s} \Im \left\{ \frac{\mathbf{s}^H \mathbf{D} \mathbf{s}}{\mathbf{s}^H \mathbf{s}} \frac{\mathbf{s}^H \mathbf{D} \boldsymbol{\Lambda} \mathbf{s}}{\mathbf{s}^H \mathbf{s}} \right\} \end{pmatrix} \end{array}$$

where WB and NB designate the wideband and narrowband terms of $\Re\{\boldsymbol{\Phi}(\boldsymbol{\eta})\}$.

On another note, from these expressions we recover the preliminary results in [44], which considered the time-delay estimation for a static system (no Doppler effect). Note that the CRBs (15), (18), (19) can be expressed as a function of the maximum SNR at the output of the MLE matched filter (11). In the static case, the CRB for the time-delay then reads

$$F_{\tau|\underline{\epsilon}}(\underline{\epsilon}) = \mathrm{SNR}_{\mathrm{out}} \times 2F_s^2 \left(\frac{\mathbf{s}^H \mathbf{V} \mathbf{s}}{\mathbf{s}^H \mathbf{s}} - \left| \frac{\mathbf{s}^H \boldsymbol{\Lambda} \mathbf{s}}{\mathbf{s}^H \mathbf{s}} \right|^2 \right), \tag{45}$$

$$F_{\tau|\underline{\epsilon}}(\underline{\epsilon}) = \mathrm{SNR}_{\mathrm{out}} \times 2F_s^2 \left(\frac{\mathbf{s}^T \mathbf{V} \mathbf{s}}{\mathbf{s}^T \mathbf{s}} \right), \tag{46}$$

for a complex $s(t)$ (45) and real $s(t)$ (46). Thus, this result can be exploited for optimal signal design, that is, to obtain a fixed-length band-limited signal $\mathbf{s}^b$ with a given fixed energy $\mathbb{E}$ (or equivalently $\mathrm{SNR}_{\mathrm{out}}$) which minimizes the CRB. We have shown in [44] that the optimal signal is related to the first eigenvector of $\mathbf{V}$, and the optimal CRB is given by

$$F_{\tau|\underline{\epsilon}}(\underline{\epsilon}) \leq 2\mathrm{SNR}_{\mathrm{out}} F_s^2 D_{1,1}, \tag{47}$$

with $\pi \leq D_{1,1} \leq \pi^2$ the largest eigenvalue of $\mathbf{V}$.

Last, from a broader perspective, the proposed CRB expressions also pave the way for the definition of new cost-functions dedicated to waveform optimization exploring the trade-off

between optimal accuracy and/or coupling when measuring time-delay and Doppler effect, and other operational constraints. For instance, they can easily be integrated to existing cost-functions used to build waveform sequences not only with good autocorrelation properties (low sidelobes level for a given energy) [45,46] or minimal peak-to-average power ratio [47], but also with optimal delay estimation accuracy, since they are fitted to any optimization method exploiting vector based cost functions [48,49].

5. Validation and Discussion

To assess the validity of the new compact closed-form CRB, a GNSS positioning example is considered [50]. In the case of GNSS, the signals broadcasted by different satellites use pseudo-orthogonal codes $s(t)$, which allow at the receiver to process different satellite signals using independent channels. Each channel estimates the time-delay and Doppler effect between the receiver and a given satellite, in order to construct a set of so-called pseudoranges and pseudorange rates, which in turn are used to solve a multilateration problem to find the receiver's position, velocity and timing. If we omit the navigation data message (i.e., assuming data wipe-off or a pilot channel) a generic signal received from a GNSS satellite, at the output of the Hilbert filter, can be expressed as in (9) and (17).

5.1. Synthetic Signal

We first consider a simulated GNSS band-limited signal corresponding to a GPS L1 C/A PRN code of length 1023. As a result that GNSS codes are real, we compute the CRB using (38). The CRB and the corresponding MLE in (10), obtained from 1000 Monte Carlo (MC) runs with $\alpha = ((1+j)/\sqrt{2})\sqrt{\text{SNR}_{\text{in}}}$, are shown in Figure 1 (top). Since (9) belongs to the class of conditional signal models [16], the MLE converges to the CRB at high SNR [17], which confirms the exactness of the CRB. This CRB is further validated by comparing the ambiguity function and its 2nd order Taylor expansion (14) in Figure 1 (bottom), where the perfect match also proves its exactness.

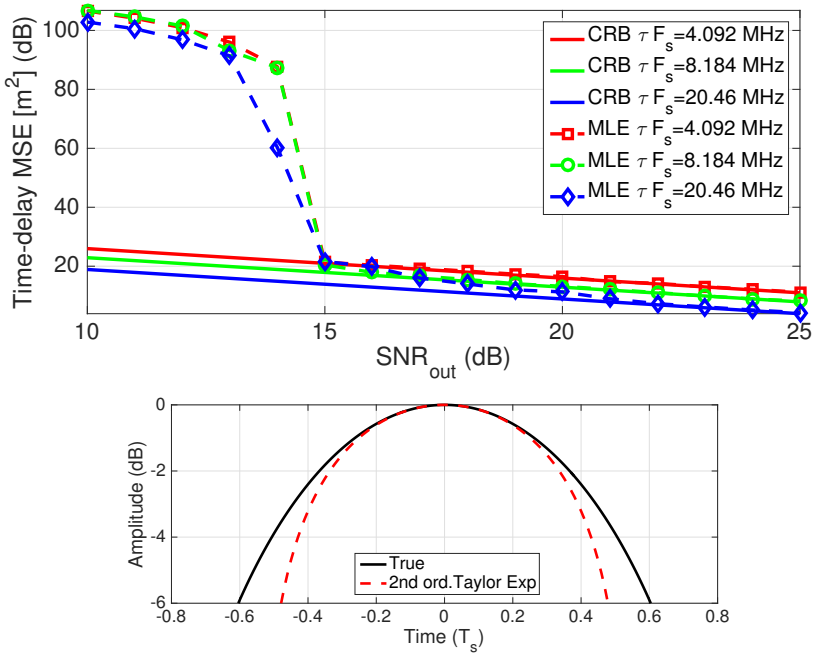

Figure 1. (**Top**) Time-delay Cramér–Rao bound (CRB) and maximum likelihood estimator (MLE) for the GPS L1 C/A PRN code (synthetic signal experiment); (**Bottom**) ambiguity function and the corresponding 2nd order Taylor expansion for the time-delay estimation of a GPS L1 C/A PRN code (synthetic signal experiment), with $F_s = 1/T_s = 1.023$ MHz (chip frequency).

5.2. Real-Life GPS Data Experiment

The proposed CRB expression was also validated in a real-life GPS scenario. The signal acquisition was performed using a static L1 frequency patch antenna in open sky conditions, and recorded using an USRP X310 at $F_s = 20$ MHz. To test standard front-end configurations, such a signal was converted to the equivalent $F_s = 5$ MHz and $F_s = 2.5$ MHz signals by averaging and decimating 4 and 8 samples, respectively. In a real-life data test it is not possible to perform MC runs, therefore the MSE was obtained via 100 different correlations, each one using a coherent integration time of 10 ms (i.e., $\mathbf{s}(\boldsymbol{\eta})$ being 10 GPS L1 C/A PRN codes of length 1 ms), and separated by 20 ms. This leads to an overall observation interval of 1s during which the hypothesis of relative uniform radial movements (4) is regarded as valid [51]. For completeness, the scenario details on the satellites in view (PRN Id), their corresponding SNR_{out} (dB), Doppler shift (Hz), elevation (°) and azimuth (°), are given in Table 1. The time-delay and Doppler frequency shift of the GPS satellite signals were obtained with the MLE in (10), where a time-delay resolution of 0.0002 chips (0.06 m) and a Doppler frequency shift resolution of 0.1 Hz were considered. Firstly, to enforce the hypothesis of relative uniform radial movements (4), the dynamics of the signal was removed by fitting a 2nd order polynomial. Secondly, notice that the SNR_{out} taken into account is estimated, and thus it is a random variable whose variance decreases with the actual SNR_{out} [35]. These results are shown in Figure 2 for the time-delay (top) and Doppler (bottom), which again validate the CRB expression at sufficiently high SNR_{out}. As highlighted by MC simulations in Figure 1, the SNR threshold for the delay estimation increases with F_s.

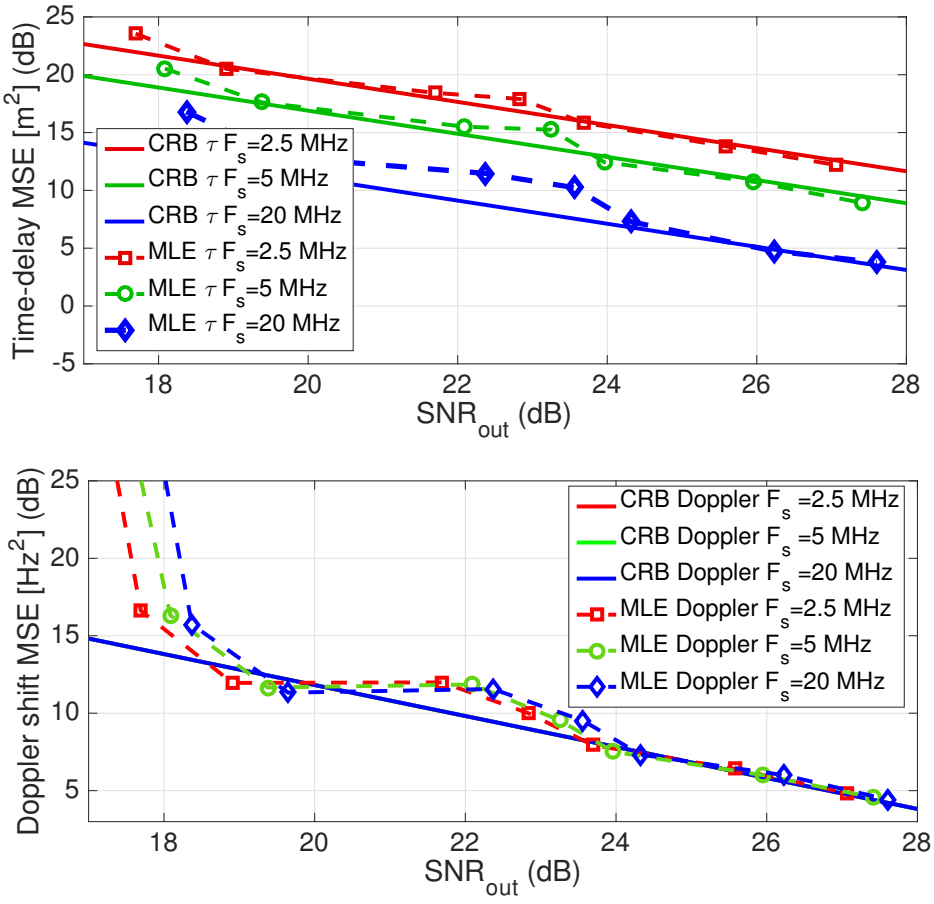

Figure 2. Time-delay (**Top**) and Doppler frequency shift (**Bottom**) CRB and MLE for a real-life GPS L1 C/A signal and different sampling rates: 2.5 MHz, 5 MHz and 20 MHz.

Table 1. Real-life GPS scenario: satellites in view (PRN Id), SNR_{out} (dB), Doppler shift (Hz), elevation (°) and azimuth (°). Data were collected on 22 April 2015, GPS week number 1841, 16:07-16:10 (UTC).

PRN Id	SNR_{out}	Doppler	Elev	Azim
31	17.7	3170	19.3	−50.6
14	18.9	−490	44.8	−95.3
2	21.7	930	28.6	86.7
24	22.8	−2950	34.1	133
25	23.7	480	70.7	−41.7
29	25.6	2480	51.3	−162.7
12	27.1	−1780	53.9	56

6. Conclusions

In this contribution, a new compact closed-form CRB expression for the delay-Doppler estimation of a generic band-limited signal has been derived, which may be exploited in a variety of remote sensing applications, i.e., navigation, radar, sonar, GNSS-R. Such a compact CRB only depends on the baseband signal samples, therefore it is especially easy to use. This generalizes known results on both wideband signals and narrowband signals where the impact of the Doppler effect into the baseband signal is not taken into account. In addition, general compact closed-form CRB expressions for the amplitude and phase have been introduced. The validity of the CRB has been assessed in a navigation example with both synthetic and measured signals. The comparison of the MLE obtained through Monte Carlo and the closed-form CRB allowed to proof the exactness of the proposed CRB. Indeed, as expected, the MLE converges to the CRB at high SNR (i.e., a known result for the Gaussian CSM). In addition, for the synthetic signal analysis, the perfect match of the ambiguity function and its 2nd order Taylor expansion also proves its exactness.

As outlooks, in addition to the performance limit characterization, these appealing closed-form CRBs, which depend only on the baseband samples' vector, pave the way for the definition of new cost-functions dedicated to waveform optimization exploring the trade-off between optimal accuracy and/or coupling when measuring time-delay and Doppler effect, and other operational constraints. For instance, they can easily be integrated to existing cost-functions used to build waveform sequences not only with good autocorrelation properties (low sidelobes level for given energy) [45,46] or minimal peak-to-average power ratio [47], but also with optimal delay estimation accuracy, since they are fitted to any optimization method exploiting vector based cost functions [48,49].

Author Contributions: Conceptualization, J.V.-V., F.V. and E.C.; methodology, F.V and E.C.; software, P.D. and E.C.; validation, P.D., J.V.-V. and E.C.; formal analysis, F.V. and E.C.; investigation, P.D., J.V.-V. and E.C; resources, L.D. and E.C.; writing—original draft preparation, P.D., J.V.-V. and E.C; writing—review and editing, F.V. and E.C.; supervision, F.V. and E.C.; project administration, L.D. and E.C.; funding acquisition, L.D. and E.C. All authors have read and agreed to the published version of the manuscript.

Funding: This research was partially supported by the DGA/AID projects (2019.65.0068.00.470.75.01, 2018.60.0072.00.470.75.01).

Conflicts of Interest: The authors declare no conflict of interest.

Appendix A. Analytic (Compact) Expression of $\Re\{\mathbf{\Phi}(\boldsymbol{\eta})\}$

Considering the model in (9), the CRB for the parameter vector $\boldsymbol{\eta} = (\tau, b)^T$ is given by (15) [34,35]. Then, the main goal is to obtain an analytic (compact) expression of $\Re\{\mathbf{\Phi}(\boldsymbol{\eta})\}$, which is not available in the literature for a generic delayed and dilated band-limited signal model. Notice that the standard

solution in the literature considers the narrowband signal model. Recall that $\Re\{\mathbf{\Phi}(\boldsymbol{\eta})\}$ can be expressed in the convenient form (24)

$$\Re\{\mathbf{\Phi}(\boldsymbol{\eta})\} = \Re\left\{\frac{\partial \mathbf{a}(\boldsymbol{\eta})}{\partial \boldsymbol{\eta}^T}^H \frac{\partial \mathbf{a}(\boldsymbol{\eta})}{\partial \boldsymbol{\eta}^T} - \frac{1}{\|\mathbf{a}(\boldsymbol{\eta})\|^2}\left(\mathbf{a}(\boldsymbol{\eta})^H \frac{\partial \mathbf{a}(\boldsymbol{\eta})}{\partial \boldsymbol{\eta}^T}\right)^H \left(\mathbf{a}(\boldsymbol{\eta})^H \frac{\partial \mathbf{a}(\boldsymbol{\eta})}{\partial \boldsymbol{\eta}^T}\right)\right\}.$$

Appendix A.1. Computing the Terms in $\mathbf{\Phi}(\boldsymbol{\eta})$

Considering the observation model in (6) and (9),

$$a(t;\boldsymbol{\eta}) = s\left((1-b)(t-\tau)\right)e^{-j\omega_c b(t-\tau)} = s(t;\boldsymbol{\eta})\,e^{-j\omega_c b(t-\tau)}, \tag{A1}$$

then we can compute the derivative w.r.t. $\boldsymbol{\eta}$, $\left(\frac{\partial a(t;\boldsymbol{\eta})}{\partial \tau}, \frac{\partial a(t;\boldsymbol{\eta})}{\partial b}\right)^T$ as

$$\begin{pmatrix} \frac{\partial a(t;\boldsymbol{\eta})}{\partial \tau} \\ \frac{\partial a(t;\boldsymbol{\eta})}{\partial b} \end{pmatrix} = -\begin{pmatrix} -j\omega_c b s(t;\boldsymbol{\eta}) + (1-b)\,s^{(1)}(t;\boldsymbol{\eta}) \\ j\omega_c (t-\tau)\,s(t;\boldsymbol{\eta}) + (t-\tau)\,s^{(1)}(t;\boldsymbol{\eta}) \end{pmatrix} e^{-j\omega_c b(t-\tau)},$$

where $s^{(1)}(t) = \frac{ds(t)}{dt}$. This can be written in a convenient matrix form as

$$\frac{\partial a(t;\boldsymbol{\eta})}{\partial \boldsymbol{\eta}} = -\mathbf{Q}\boldsymbol{\vartheta}(t;\boldsymbol{\eta})\,e^{-j\omega_c b(t-\tau)}, \tag{A2}$$

where

$$\mathbf{Q} = \begin{bmatrix} -j\omega_c b & 0 & (1-b) & 0 \\ 0 & j\omega_c & 0 & 1 \end{bmatrix}, \boldsymbol{\vartheta}(t;\boldsymbol{\eta}) = \begin{pmatrix} s(t;\boldsymbol{\eta}) \\ (t-\tau)\,s(t;\boldsymbol{\eta}) \\ s^{(1)}(t;\boldsymbol{\eta}) \\ (t-\tau)\,s^{(1)}(t;\boldsymbol{\eta}) \end{pmatrix}.$$

Then, the derivative of $\mathbf{a}^T(\boldsymbol{\eta})$ ($t = nT_s$, with samples $N_1' \le n \le N_2'$) w.r.t. $\boldsymbol{\eta}$ is

$$\begin{aligned}\frac{\partial \mathbf{a}^T(\boldsymbol{\eta})}{\partial \boldsymbol{\eta}} &= \begin{bmatrix} \cdots & \frac{\partial a(nT_s;\boldsymbol{\eta})}{\partial \boldsymbol{\eta}} & \cdots \end{bmatrix}_{N_1' \le n \le N_2'} = \begin{bmatrix} \cdots & -\mathbf{Q}\boldsymbol{\vartheta}(nT_s;\boldsymbol{\eta})\,e^{-j\omega_c b(nT_s-\tau)} & \cdots \end{bmatrix}_{N_1' \le n \le N_2'} \\ &= -\mathbf{Q}\begin{bmatrix} \cdots & \boldsymbol{\vartheta}(nT_s;\boldsymbol{\eta})\,e^{-j\omega_c b(nT_s-\tau)} & \cdots \end{bmatrix}_{N_1' \le n \le N_2'},\end{aligned}$$

and because the complex conjugate of vector $\mathbf{a}(\boldsymbol{\eta})$ is given by

$$\mathbf{a}^*(\boldsymbol{\eta}) = \begin{pmatrix} \vdots \\ a(nT_s;\boldsymbol{\eta}) \\ \vdots \end{pmatrix}^*_{N_1' \le n \le N_2'} = \begin{pmatrix} \vdots \\ s(nT_s;\boldsymbol{\eta})^*\,e^{j\omega_c b(nT_s-\tau)} \\ \vdots \end{pmatrix}_{N_1' \le n \le N_2'}$$

we have that

$$\frac{\partial \mathbf{a}^T(\boldsymbol{\eta})}{\partial \boldsymbol{\eta}}\mathbf{a}^*(\boldsymbol{\eta}) = -\mathbf{Q}\left(\sum_{n=N_1'}^{N_2'} \boldsymbol{\vartheta}(nT_s;\boldsymbol{\eta})\,s(nT_s;\boldsymbol{\eta})^*\right).$$

Given the following equalities,

$$\frac{\partial \mathbf{a}(\boldsymbol{\eta})}{\partial \boldsymbol{\eta}^T}^H = \left(\frac{\partial \mathbf{a}(\boldsymbol{\eta})^T}{\partial \boldsymbol{\eta}}\right)^*, \quad \frac{\partial \mathbf{a}(\boldsymbol{\eta})}{\partial \boldsymbol{\eta}^T} = \left(\frac{\partial \mathbf{a}(\boldsymbol{\eta})^T}{\partial \boldsymbol{\eta}}\right)^T,$$

we can write that

$$\frac{\partial \mathbf{a}(\boldsymbol{\eta})}{\partial \boldsymbol{\eta}^T}^H \frac{\partial \mathbf{a}(\boldsymbol{\eta})}{\partial \boldsymbol{\eta}^T} = \mathbf{Q}^* \left(\sum_{n=N_1'}^{N_2'} \boldsymbol{\vartheta}(nT_s;\boldsymbol{\eta})^* \boldsymbol{\vartheta}^T(nT_s;\boldsymbol{\eta}) \right) \mathbf{Q}^T.$$

Finally, we have all the terms in (24),

$$\mathbf{a}^H(\boldsymbol{\eta}) \frac{\partial \mathbf{a}(\boldsymbol{\eta})}{\partial \boldsymbol{\eta}^T} = -\left(\sum_{n=N_1'}^{N_2'} \boldsymbol{\vartheta}(nT_s;\boldsymbol{\eta}) s(nT_s;\boldsymbol{\eta})^* \right)^T \mathbf{Q}^T, \tag{A3}$$

$$\frac{\partial \mathbf{a}(\boldsymbol{\eta})}{\partial \boldsymbol{\eta}^T}^H \frac{\partial \mathbf{a}(\boldsymbol{\eta})}{\partial \boldsymbol{\eta}^T} = \left(\mathbf{Q} \left(\sum_{n=N_1'}^{N_2'} \boldsymbol{\vartheta}(nT_s;\boldsymbol{\eta}) \boldsymbol{\vartheta}^H(nT_s;\boldsymbol{\eta}) \right) \mathbf{Q}^H \right)^*, \tag{A4}$$

$$\|\mathbf{a}(\boldsymbol{\eta})\|^2 = \sum_{n=N_1'}^{N_2'} |s(nT_s;\boldsymbol{\eta})|^2, \tag{A5}$$

but these expressions are not yet in a compact form.

Appendix A.2. Integral Form of the Inner Terms in (A3) and (A4)

Note that if $x(t)$ is a band-limited signal with $B \leq F_s$, then $x^{(1)}(t)$, $tx(t)$ and $tx^{(1)}(t)$ are also band-limited with $B \leq F_s$. In this case, we can write

$$x(t) \rightleftharpoons x(f) = T_s \sum_{-\infty}^{+\infty} x(nT_s) e^{-j2\pi f n T_s}, \tag{A6}$$

$$x^{(1)}(t) \rightleftharpoons (j2\pi f) x(f), \tag{A7}$$

$$\Downarrow$$

$$\left| \begin{array}{l} \int_{-\infty}^{+\infty} tx(t) e^{-j2\pi f t} dt = \frac{j}{2\pi} \frac{dx(f)}{df} = T_s \sum_{-\infty}^{+\infty} (nT_s) x(nT_s) e^{-j2\pi f n T_s} \\ \int_{-\infty}^{+\infty} tx^{(1)}(t) e^{-j2\pi f t} dt = \frac{j}{2\pi} \frac{d(j2\pi f x(f))}{df} = -x(f) - f\frac{dx(f)}{df} = T_s \sum_{-\infty}^{+\infty} (nT_s) x^{(1)}(nT_s) e^{-j2\pi f n T_s} \end{array} \right. \tag{A8}$$

If $s(t)$ is a band-limited signal, $\boldsymbol{\vartheta}(t;\boldsymbol{\eta})$ is also band-limited (see above) and we can write the inner term in (A3) as,

$$\lim_{(N_1',N_2') \to (-\infty,+\infty)} T_s \sum_{n=N_1'}^{N_2'} \boldsymbol{\vartheta}(nT_s;\boldsymbol{\eta}) s(nT_s;\boldsymbol{\eta})^* = \int_{-\infty}^{+\infty} \boldsymbol{\vartheta}(t;\boldsymbol{\eta}) s(t;\boldsymbol{\eta})^* dt$$

$$= \mathbf{w} = \begin{pmatrix} w_1 = \int_{-\infty}^{+\infty} |s(t;\boldsymbol{\eta})|^2 dt \\ w_2 = \int_{-\infty}^{+\infty} (t-\tau) |s(t;\boldsymbol{\eta})|^2 dt \\ w_3 = \int_{-\infty}^{+\infty} s^{(1)}(t;\boldsymbol{\eta}) s(t;\boldsymbol{\eta})^* dt \\ w_4 = \int_{-\infty}^{+\infty} (t-\tau) s^{(1)}(t;\boldsymbol{\eta}) s(t;\boldsymbol{\eta})^* dt \end{pmatrix}, \tag{A9}$$

and we can do the same for the inner term in (A4),

$$\begin{aligned}\lim_{\left(N_1',N_2'\right)\to(-\infty,+\infty)} T_s \sum_{n=N_1'}^{N_2'} \boldsymbol{\vartheta}\left(nT_s;\boldsymbol{\eta}\right)\boldsymbol{\vartheta}^H\left(nT_s;\boldsymbol{\eta}\right) &= \int_{-\infty}^{+\infty} \boldsymbol{\vartheta}\left(t;\boldsymbol{\eta}\right)\boldsymbol{\vartheta}\left(t;\boldsymbol{\eta}\right)^H dt \\ &= \mathbf{W} = \begin{bmatrix} w_1 & w_2^* & w_3^* & w_4^* \\ w_2 & W_{2,2} & w_4^* & W_{4,2}^* \\ w_3 & w_4 & W_{3,3} & W_{4,3}^* \\ w_4 & W_{4,2} & W_{4,3} & W_{4,4} \end{bmatrix}\end{aligned} \tag{A10}$$

where the missing terms are defined as

$$\begin{aligned} W_{2,2} &= \int_{-\infty}^{+\infty} (t-\tau)^2 \left|s\left(t;\boldsymbol{\eta}\right)\right|^2 dt, \\ W_{3,3} &= \int_{-\infty}^{+\infty} \left|s^{(1)}\left(t;\boldsymbol{\eta}\right)\right|^2 dt, \\ W_{4,2} &= \int_{-\infty}^{+\infty} (t-\tau)^2 s^{(1)}\left(t;\boldsymbol{\eta}\right) s\left(t;\boldsymbol{\eta}\right)^* dt, \\ W_{4,3} &= \int_{-\infty}^{+\infty} (t-\tau) \left|s^{(1)}\left(t;\boldsymbol{\eta}\right)\right|^2 dt, \\ W_{4,4} &= \int_{-\infty}^{+\infty} (t-\tau)^2 \left|s^{(1)}\left(t;\boldsymbol{\eta}\right)\right|^2 dt. \end{aligned}$$

We can further work the terms in **W** as follows (with $\beta = (1-b)$):

$$\begin{aligned} w_1 &= \int_{-\infty}^{+\infty} \left|s\left(t;\boldsymbol{\eta}\right)\right|^2 dt = \int_{-\infty}^{+\infty} \left|s\left(\beta\left(t-\tau\right)\right)\right|^2 dt = \frac{1}{\beta}\int_{-\infty}^{+\infty} \left|s\left(\beta u\right)\right|^2 \beta du = \frac{1}{\beta}\int_{-\infty}^{+\infty} \left|s\left(t\right)\right|^2 dt, \\ w_2 &= \int_{-\infty}^{+\infty} (t-\tau)\left|s\left(t;\boldsymbol{\eta}\right)\right|^2 dt = \int_{-\infty}^{+\infty} (t-\tau)\left|s\left(\beta\left(t-\tau\right)\right)\right|^2 dt \\ &= \frac{1}{\beta^2}\int_{-\infty}^{+\infty} \beta u \left|s\left(\beta u\right)\right|^2 \beta du = \frac{1}{\beta^2}\int_{-\infty}^{+\infty} t\left|s\left(t\right)\right|^2 dt, \\ w_3 &= \int_{-\infty}^{+\infty} s^{(1)}\left(t;\boldsymbol{\eta}\right) s\left(t;\boldsymbol{\eta}\right)^* dt = \int_{-\infty}^{+\infty} s^{(1)}\left(\beta\left(t-\tau\right)\right) s\left(\beta\left(t-\tau\right)\right)^* dt \\ &= \frac{1}{\beta}\int_{-\infty}^{+\infty} s^{(1)}\left(\beta u\right) s\left(\beta u\right)^* \beta du = \frac{1}{\beta}\int_{-\infty}^{+\infty} s^{(1)}\left(t\right) s\left(t\right)^* dt, \\ w_4 &= \int_{-\infty}^{+\infty} (t-\tau)\, s^{(1)}\left(t;\boldsymbol{\eta}\right) s\left(t;\boldsymbol{\eta}\right)^* dt = \int_{-\infty}^{+\infty} (t-\tau)\, s^{(1)}\left(\beta\left(t-\tau\right)\right) s\left(\beta\left(t-\tau\right)\right)^* dt \\ &= \frac{1}{\beta^2}\int_{-\infty}^{+\infty} \beta u s^{(1)}\left(\beta u\right) s\left(\beta u\right)^* \beta du = \frac{1}{\beta^2}\int_{-\infty}^{+\infty} t s^{(1)}\left(t\right) s\left(t\right)^* dt, \end{aligned}$$

$$W_{2,2} = \int_{-\infty}^{+\infty} (t-\tau)^2 \left| s\left(t;\boldsymbol{\eta}\right)\right|^2 dt = \int_{-\infty}^{+\infty} (t-\tau)^2 \left| s\left(\beta\left(t-\tau\right)\right)\right|^2 dt$$
$$= \frac{1}{\beta^3}\int_{-\infty}^{+\infty} (\beta u)^2 \left| s\left(\beta u\right)\right|^2 \beta du = \frac{1}{\beta^3}\int_{-\infty}^{+\infty} t^2 \left| s\left(t\right)\right|^2 dt,$$
$$W_{3,3} = \int_{-\infty}^{+\infty} \left| s^{(1)}\left(t;\boldsymbol{\eta}\right)\right|^2 dt = \int_{-\infty}^{+\infty} \left| s^{(1)}\left(\beta\left(t-\tau\right)\right)\right|^2 dt$$
$$= \frac{1}{\beta}\int_{-\infty}^{+\infty} \left| s^{(1)}\left(\beta u\right)\right|^2 \beta du = \frac{1}{\beta}\int_{-\infty}^{+\infty} \left| s^{(1)}\left(t\right)\right|^2 dt,$$
$$W_{4,2} = \int_{-\infty}^{+\infty} (t-\tau)^2 s^{(1)}\left(t;\boldsymbol{\eta}\right) s\left(t;\boldsymbol{\eta}\right)^* dt = \int_{-\infty}^{+\infty} (t-\tau)^2 s^{(1)}\left(\beta\left(t-\tau\right)\right) s\left(\beta\left(t-\tau\right)\right)^* dt$$
$$= \frac{1}{\beta^3}\int_{-\infty}^{+\infty} (\beta u)^2 s^{(1)}\left(\beta u\right) s\left(\beta u\right)^* \beta du = \frac{1}{\beta^3}\int_{-\infty}^{+\infty} t^2 s^{(1)}\left(t\right) s\left(t\right)^* dt,$$
$$W_{4,3} = \int_{-\infty}^{+\infty} (t-\tau) \left| s^{(1)}\left(t;\boldsymbol{\eta}\right)\right|^2 dt = \int_{-\infty}^{+\infty} (t-\tau) \left| s^{(1)}\left(\beta\left(t-\tau\right)\right)\right|^2 dt$$
$$= \frac{1}{\beta^2}\int_{-\infty}^{+\infty} (\beta u) \left| s^{(1)}\left(\beta u\right)\right|^2 \beta du = \frac{1}{\beta^2}\int_{-\infty}^{+\infty} t \left| s^{(1)}\left(t\right)\right|^2 dt,$$
$$W_{4,4} = \int_{-\infty}^{+\infty} (t-\tau)^2 \left| s^{(1)}\left(t;\boldsymbol{\eta}\right)\right|^2 dt = \int_{-\infty}^{+\infty} (t-\tau)^2 \left| s^{(1)}\left(\beta\left(t-\tau\right)\right)\right|^2 dt$$
$$= \frac{1}{\beta^3}\int_{-\infty}^{+\infty} (\beta u)^2 \left| s^{(1)}\left(\beta u\right)\right|^2 \beta du = \frac{1}{\beta^3}\int_{-\infty}^{+\infty} t^2 \left| s^{(1)}\left(t\right)\right|^2 dt,$$

where

$$w_1, w_2, W_{2,2}, W_{3,3}, W_{4,3}, W_{4,4} \in \mathbb{R}. \tag{A11}$$

Appendix A.3. Rewriting (24) in Terms of **W**

Going back to the original problem in (24), we have to make appear the term T_s to exploit the previous expressions,

$$\Re\left\{\boldsymbol{\Phi}\left(\boldsymbol{\eta}\right)\right\} = F_s \Re\left\{ T_s \frac{\partial \mathbf{a}\left(\boldsymbol{\eta}\right)}{\partial \boldsymbol{\eta}^T}^H \frac{\partial \mathbf{a}\left(\boldsymbol{\eta}\right)}{\partial \boldsymbol{\eta}^T} - \frac{1}{T_s \left\|\mathbf{a}\left(\boldsymbol{\eta}\right)\right\|^2} \left(T_s \mathbf{a}\left(\boldsymbol{\eta}\right)^H \frac{\partial \mathbf{a}\left(\boldsymbol{\eta}\right)}{\partial \boldsymbol{\eta}^T}\right)^H \left(T_s \mathbf{a}\left(\boldsymbol{\eta}\right)^H \frac{\partial \mathbf{a}\left(\boldsymbol{\eta}\right)}{\partial \boldsymbol{\eta}^T}\right) \right\},$$

and then we can write (using (A3)–(A5) and (A9) and (A10)) that

$$\lim_{\left(N_1',N_2'\right)\to(-\infty,+\infty)} \Re\left\{\mathbf{\Phi}\left(\boldsymbol{\eta}\right)\right\} = F_s\Re\left\{\begin{array}{l}\left(\lim\limits_{\left(N_1',N_2'\right)\to(-\infty,+\infty)} T_s\frac{\partial\mathbf{a}(\boldsymbol{\eta})}{\partial\boldsymbol{\eta}^T}^H\frac{\partial\mathbf{a}(\boldsymbol{\eta})}{\partial\boldsymbol{\eta}^T}\right) - \\ \frac{\left(\lim\limits_{\left(N_1',N_2'\right)\to(-\infty,+\infty)} T_s\mathbf{a}(\boldsymbol{\eta})^H\frac{\partial\mathbf{a}(\boldsymbol{\eta})}{\partial\boldsymbol{\eta}^T}\right)^H}{\lim\limits_{\left(N_1',N_2'\right)\to(-\infty,+\infty)} T_s\|\mathbf{a}(\boldsymbol{\eta})\|^2} \\ \times\left(\lim\limits_{\left(N_1',N_2'\right)\to(-\infty,+\infty)} T_s\mathbf{a}\left(\boldsymbol{\eta}\right)^H\frac{\partial\mathbf{a}(\boldsymbol{\eta})}{\partial\boldsymbol{\eta}^T}\right)\end{array}\right\}$$

$$= F_s\Re\left\{\left(\mathbf{QWQ}^H\right)^* - \frac{\left(-\left(\mathbf{w}\right)^T\mathbf{Q}^T\right)^H\left(-\left(\mathbf{w}\right)^T\mathbf{Q}^T\right)}{w_1}\right\}, \tag{A12}$$

that is

$$\lim_{\min\left(N_1',N_2'\right)\to\infty} \mathrm{Re}\left\{\mathbf{\Phi}\left(\boldsymbol{\eta}\right)\right\} = F_s\,\mathrm{Re}\left\{\mathbf{QWQ}^H - \frac{\left(\mathbf{Qw}\right)\left(\mathbf{Qw}\right)^H}{w_1}\right\}. \tag{A13}$$

Appendix A.4. Computing $\mathbf{QWQ}^H$, $\mathbf{Qw}$ *and* $\frac{(\mathbf{Qw})(\mathbf{Qw})^H}{w_1}$

The term is $\mathbf{QWQ}^H$ given by

$$\mathbf{QWQ}^H = \begin{bmatrix} -j\omega_c b & 0 & (1-b) & 0 \\ 0 & j\omega_c & 0 & 1 \end{bmatrix}\begin{bmatrix} w_1 & w_2^* & w_3^* & w_4^* \\ w_2 & W_{2,2} & w_4^* & W_{4,2}^* \\ w_3 & w_4 & W_{3,3} & W_{4,3}^* \\ w_4 & W_{4,2} & W_{4,3} & W_{4,4} \end{bmatrix}\begin{bmatrix} j\omega_c b & 0 \\ 0 & -j\omega_c \\ (1-b) & 0 \\ 0 & 1 \end{bmatrix},$$

$$\begin{aligned}\left(\mathbf{QWQ}^H\right)_{1,1} &= (1-b)^2 W_{3,3} + (\omega_c b)^2 w_1 + 2(1-b)(\omega_c b)\,\mathrm{Re}\left\{jw_3\right\},\\ \left(\mathbf{QWQ}^H\right)_{1,2} &= \begin{pmatrix} (-j\omega_c b)(-j\omega_c)w_2^* + (1-b)(-j\omega_c)w_4 \\ +(-j\omega_c b)w_4^* + (1-b)W_{4,3}^* \end{pmatrix} = \left(\mathbf{QWQ}^H\right)_{2,1}^*,\\ \left(\mathbf{QWQ}^H\right)_{2,2} &= \omega_c^2 W_{2,2} - 2\omega_c\,\mathrm{Re}\left\{jW_{4,2}\right\} + W_{4,4},\end{aligned}$$

and the term $\mathbf{Qw}$ is given by

$$\mathbf{Qw} = \begin{bmatrix} -j\omega_c b & 0 & (1-b) & 0 \\ 0 & j\omega_c & 0 & 1 \end{bmatrix}\mathbf{w} = \begin{pmatrix} -j\omega_c b w_1 + (1-b)w_3 \\ j\omega_c w_2 + w_4 \end{pmatrix},$$

which leads to the following

$$\begin{aligned}\left(\frac{\left(\mathbf{Qw}\right)\left(\mathbf{Qw}\right)^H}{w_1}\right)_{1,1} &= (\omega_c b)^2 w_1 + \frac{(1-b)^2|w_3|^2}{w_1} + 2(1-b)\,\omega_c b\,\mathrm{Re}\left\{jw_3\right\},\\ \left(\frac{\left(\mathbf{Qw}\right)\left(\mathbf{Qw}\right)^H}{w_1}\right)_{1,2} &= \begin{pmatrix} j\omega_c(j\omega_c b)w_2 + (j\omega_c b)w_4 \\ +(j\omega_c)(1-b)\frac{w_2 w_3^*}{w_1} + (1-b)\frac{w_4 w_3^*}{w_1} \end{pmatrix}^*,\\ \left(\frac{\left(\mathbf{Qw}\right)\left(\mathbf{Qw}\right)^H}{w_1}\right)_{2,2} &= \omega_c^2\frac{w_2^2}{w_1} + \frac{|w_4|^2}{w_1} + 2\omega_c\frac{w_2\,\mathrm{Im}\left\{w_4\right\}}{w_1}.\end{aligned}$$

Appendix A.5. Analytic Expression of $\Re\{\mathbf{\Phi}(\boldsymbol{\eta})\}$

Finally, taking into account (A11), then (A13) can be expressed as

$$\left(\lim_{\min\left(N_1',N_2'\right)\to\infty}\Re\{\mathbf{\Phi}(\boldsymbol{\eta})\}\right)_{1,1}=F_s(1-b)^2\left(W_{3,3}-\frac{|w_3|^2}{w_1}\right),$$

$$\left(\lim_{\min\left(N_1',N_2'\right)\to\infty}\Re\{\mathbf{\Phi}(\boldsymbol{\eta})\}\right)_{1,2}=F_s(1-b)\begin{pmatrix}\omega_c\,\mathrm{Im}\left\{w_4-\frac{w_3w_2}{w_1}\right\}\\-\frac{1}{w_1}\,\mathrm{Re}\left\{w_3w_4^*\right\}+W_{4,3}\end{pmatrix},$$

$$\left(\lim_{\min\left(N_1',N_2'\right)\to\infty}\Re\{\mathbf{\Phi}(\boldsymbol{\eta})\}\right)_{2,2}=F_s\begin{pmatrix}\omega_c^2\left(W_{2,2}-\frac{w_2^2}{w_1}\right)+W_{4,4}-\frac{|w_4|^2}{w_1}\\+2\omega_c\,\mathrm{Im}\left\{W_{4,2}-\frac{w_2w_4}{w_1}\right\}\end{pmatrix}.$$

where the integral form of the different terms is detailed after (A10).

Appendix A.6. Analytic Expression of $\Re\{\mathbf{\Phi}(\boldsymbol{\eta})\}$ *when* $s(t)$ *is a Real Signal*

Let us first recall that if $s(t)\rightleftharpoons s(f)$, then $s^{(1)}(t)\rightleftharpoons j2\pi fs(f)$, $ts(t)\rightleftharpoons\frac{j}{2\pi}\frac{ds(f)}{df}$ and $ts^{(1)}(t)\rightleftharpoons -s(f)-f\frac{ds(f)}{df}$. If $s(t)$ is a real signal, in addition we have that $s(-f)=s^*(f)$ and $\frac{ds(-f)}{df}=-\left(\frac{ds(f)}{df}\right)^*$, which directly leads to $w_3=0$ and $W_{4,2},w_4\in\mathbb{R}$. We detail this statement in the sequel,

$$w_3=\int_{-\infty}^{+\infty}s^{(1)}(t)\,s(t)\,dt=\int_{-\infty}^{+\infty}(j2\pi f)\,s(f)\,s(f)^*\,df=j2\pi\int_{-\frac{F_s}{2}}^{\frac{F_s}{2}}f\,|s(f)|^2\,df=0,$$

$$W_{4,2}=\frac{1}{(1-b)^3}\int_{-\infty}^{+\infty}\left(ts^{(1)}(t)\right)(ts(t))^*\,dt=\frac{1}{(1-b)^3}\int_{-\frac{F_s}{2}}^{\frac{F_s}{2}}\left(-s(f)-f\frac{ds(f)}{df}\right)\left(\frac{j}{2\pi}\frac{ds(f)}{df}\right)^*df$$

$$=\frac{j}{2\pi}\frac{1}{(1-b)^3}\int_{-\frac{F_s}{2}}^{\frac{F_s}{2}}s(f)\,\frac{ds(f)}{df}^*df=\frac{1}{\pi(1-b)^3}\Im\left\{\int_0^{\frac{F_s}{2}}\left(\frac{ds(f)}{df}\right)s^*(f)\,df\right\},$$

$$w_4=\frac{1}{(1-b)^2}\int_{-\infty}^{+\infty}s^{(1)}(t)\,(ts(t))\,dt=\frac{1}{(1-b)^2}\int_{-\frac{F_s}{2}}^{\frac{F_s}{2}}(j2\pi fs(f))\left(\frac{j}{2\pi}\frac{ds(f)}{df}\right)^*df$$

$$=\frac{1}{(1-b)^2}\int_{-\frac{F_s}{2}}^{\frac{F_s}{2}}fs(f)\,\frac{ds(f)}{df}^*df=\frac{2}{(1-b)^2}\Re\left\{\int_0^{\frac{F_s}{2}}f\left(\frac{ds(f)}{df}\right)s(f)^*\,df\right\}.$$

Taking into account this into (24) leads to the simplified expression,

$$\lim_{\min\left(N_1',N_2'\right)\to\infty}\mathrm{Re}\{\mathbf{\Phi}(\boldsymbol{\eta})\}=F_s\begin{bmatrix}(1-b)^2W_{3,3}&(1-b)W_{4,3}\\(1-b)W_{4,3}&\omega_c^2\left(W_{2,2}-\frac{w_2^2}{w_1}\right)+W_{4,4}-\frac{w_4^2}{w_1}\end{bmatrix}.\tag{A14}$$

Appendix B. Computation of the Different Terms in the CRB Expression (25)–(26)

Recall again that if $s(t) \rightleftharpoons s(f)$, then $s^{(1)}(t) \rightleftharpoons j2\pi f s(f)$, $ts(t) \rightleftharpoons \frac{j}{2\pi}\frac{ds(f)}{df}$ and $ts^{(1)}(t) \rightleftharpoons -s(f) - f\frac{ds(f)}{df}$. Moreover, $s(f) = \frac{1}{F_s}\sum_{N_1}^{N_2} s(nT_s)\, e^{-j2\pi\frac{f}{F_s}n}$ and the derivative is given by $\frac{ds(f)}{df} = \frac{-j2\pi}{F_s^2}\sum_{N_1}^{N_2} ns(nT_s)\, e^{-j2\pi\frac{f}{F_s}n}$, which allow to operate with the signal samples. The 9 terms in the CRB (i.e., w_1, w_2, w_3, w_4, $W_{2,2}$, $W_{3,3}$, $W_{4,2}$, $W_{4,3}$ and $W_{4,4}$) are computed as follows (with $\beta = (1-b)$):

$$\beta w_1 = \int_{-\infty}^{+\infty} s(t)\, s(t)^*\, dt = \int_{-\frac{F_s}{2}}^{\frac{F_s}{2}} s(f)\, s(f)^*\, df = \frac{1}{F_s}\mathbf{s}^H\left(\int_{-\frac{1}{2}}^{\frac{1}{2}} \boldsymbol{v}(f)\, \boldsymbol{v}^H(f)\, df\right)\mathbf{s} = \frac{1}{F_s}\mathbf{s}^H\mathbf{s},$$

$$\begin{aligned}\beta^2 w_2 &= \int_{-\infty}^{+\infty} s(t)\,(ts(t))^*\, dt = \int_{-\frac{F_s}{2}}^{\frac{F_s}{2}} s(f)\left(\frac{j}{2\pi}\frac{ds(f)}{df}\right)^* df \\ &= \frac{1}{F_s^2}\int_{-\frac{1}{2}}^{\frac{1}{2}} \left((\mathbf{Ds})^H \boldsymbol{v}(f)\right)\left(\boldsymbol{v}^H(f)\,\mathbf{s}\right) df = \frac{1}{F_s^2}\mathbf{s}^H\left(\mathbf{D}^H\int_{-\frac{1}{2}}^{\frac{1}{2}} \boldsymbol{v}(f)\, \boldsymbol{v}^H(f)\, df\right)\mathbf{s} = \frac{1}{F_s^2}\mathbf{s}^H\mathbf{Ds},\end{aligned}$$

$$\beta w_3 = \int_{-\infty}^{+\infty} s^{(1)}(t)\, s(t)^*\, dt = \int_{-\frac{F_s}{2}}^{\frac{F_s}{2}} (j2\pi f)\,|s(f)|^2\, df = \int_{-\frac{1}{2}}^{\frac{1}{2}} (j2\pi f)\left|\boldsymbol{v}^H(f)\,\mathbf{s}\right|^2 df = \mathbf{s}^H\boldsymbol{\Lambda}\mathbf{s},$$

$$\begin{aligned}\beta^2 w_4 &= \int_{-\infty}^{+\infty} s^{(1)}(t)\,(ts(t))^*\, dt = \int_{-\frac{F_s}{2}}^{\frac{F_s}{2}} (j2\pi f)\, s(f)\left(\frac{j}{2\pi}\frac{ds(f)}{df}\right)^* df \\ &= \frac{1}{F_s}\int_{-\frac{1}{2}}^{\frac{1}{2}} (j2\pi f)\left(\boldsymbol{v}^H(f)\,\mathbf{s}\right)\left((\mathbf{Ds})^H \boldsymbol{v}(f)\right) df = \frac{1}{F_s}\mathbf{s}^H\mathbf{D}^H\left(j2\pi\int_{-\frac{1}{2}}^{\frac{1}{2}} f\boldsymbol{v}(f)\, \boldsymbol{v}^H(f)\, df\right)\mathbf{s} \\ &= \frac{1}{F_s}\mathbf{s}^H\mathbf{D}\boldsymbol{\Lambda}\mathbf{s},\end{aligned}$$

$$\begin{aligned}\beta^3 W_{2,2} &= \int_{-\infty}^{+\infty} |ts(t)|^2\, dt = \int_{-\frac{F_s}{2}}^{\frac{F_s}{2}} \left|\frac{j}{2\pi}\frac{ds(f)}{df}\right|^2 df = \frac{1}{F_s^3}\int_{-\frac{1}{2}}^{\frac{1}{2}} \left|\boldsymbol{v}^H(f)\,(\mathbf{Ds})\right|^2 df \\ &= \frac{1}{F_s^3}\mathbf{s}^H\mathbf{D}^H\left(\int_{-\frac{1}{2}}^{\frac{1}{2}} \boldsymbol{v}(f)\, \boldsymbol{v}^H(f)\, df\right)\mathbf{Ds} = \frac{1}{F_s^3}\mathbf{s}^H\mathbf{D}^2\mathbf{s},\end{aligned}$$

$$\beta W_{3,3} = \int_{-\infty}^{+\infty} \left|s^{(1)}(t)\right|^2 dt = \int_{-\frac{F_s}{2}}^{\frac{F_s}{2}} |(j2\pi f)\, s(f)|^2\, df = F_s\int_{-\frac{1}{2}}^{\frac{1}{2}} (2\pi f)^2\left|\boldsymbol{v}^H(f)\,\mathbf{s}\right|^2 df = F_s\mathbf{s}^H\mathbf{Vs},$$

$$\begin{aligned}\beta^3 W_{4,2} &= \int_{-\infty}^{+\infty} \left(ts^{(1)}(t)\right)(ts(t))^*\, dt = \int_{-\frac{F_s}{2}}^{\frac{F_s}{2}} \left(-s(f) - f\frac{ds(f)}{df}\right)\left(\frac{j}{2\pi}\frac{ds(f)}{df}\right)^* df \\ &= \frac{-1}{F_s^2}\int_{-\frac{1}{2}}^{\frac{1}{2}} \left(\mathbf{s}^T\boldsymbol{v}^*(f)\right)\left((\mathbf{Ds})^H \boldsymbol{v}(f)\right) df + \frac{j2\pi}{F_s^2}\int_{-\frac{1}{2}}^{\frac{1}{2}} f\left|(\mathbf{Ds})^H \boldsymbol{v}(f)\right|^2 df \\ &= \frac{-1}{F_s^2}\mathbf{s}^H\mathbf{D}^H\left(\int_{-\frac{1}{2}}^{\frac{1}{2}} \boldsymbol{v}(f)\, \boldsymbol{v}^H(f)\, df\right)\mathbf{s} + \frac{1}{F_s^2}\mathbf{s}^H\mathbf{D}^H\left(j2\pi\int_{-\frac{1}{2}}^{\frac{1}{2}} f\boldsymbol{v}(f)\, \boldsymbol{v}(f)^H\, df\right)\mathbf{Ds} \\ &= \frac{1}{F_s^2}\left(\mathbf{s}^H\mathbf{D}\boldsymbol{\Lambda}\mathbf{Ds} - \mathbf{s}^H\mathbf{Ds}\right),\end{aligned}$$

$$\beta^2 W_{4,3} = \int_{-\infty}^{+\infty} \left(ts^{(1)}(t) \right) s^{(1)}(t)^* \, dt = j2\pi \int_{-\frac{F_s}{2}}^{\frac{F_s}{2}} f \left| s(f) \right|^2 df + j2\pi \int_{-\frac{F_s}{2}}^{\frac{F_s}{2}} f^2 \frac{ds(f)}{df} \left(s(f)^* \right) df$$
$$= \int_{-\frac{1}{2}}^{\frac{1}{2}} j2\pi f \left| \mathbf{s}^H \boldsymbol{v}(f) \right|^2 df + 4\pi^2 \int_{-\frac{1}{2}}^{\frac{1}{2}} f^2 \left(\boldsymbol{v}^H(f) (\mathbf{Ds}) \right) \left(\mathbf{s}^H \boldsymbol{v}(f) \right) df = \mathbf{s}^H \mathbf{\Lambda s} + \mathbf{s}^H \mathbf{V Ds},$$

$$\beta^3 W_{4,4} = \int_{-\infty}^{+\infty} \left| ts^{(1)}(t) \right|^2 dt = \int_{-\frac{F_s}{2}}^{\frac{F_s}{2}} \left| s(f) \right|^2 df + \int_{-\frac{F_s}{2}}^{\frac{F_s}{2}} f^2 \left| \frac{ds(f)}{df} \right|^2 df + 2\Re \left\{ \int_{-\frac{F_s}{2}}^{\frac{F_s}{2}} f \frac{ds(f)}{df} s(f)^* \right\} df$$
$$= \frac{1}{F_s} \mathbf{s}^H \mathbf{s} + \frac{1}{F_s} \mathbf{s}^H \mathbf{D} \left(4\pi^2 \int_{-\frac{1}{2}}^{\frac{1}{2}} f^2 \boldsymbol{v}(f) \boldsymbol{v}(f)^H df \right) \mathbf{Ds} - \frac{2}{F_s} \Re \left\{ \mathbf{s}^H \left(j2\pi \int_{-\frac{1}{2}}^{\frac{1}{2}} f \boldsymbol{v}(f) \boldsymbol{v}(f)^H df \right) \mathbf{Ds} \right\}$$
$$= \frac{1}{F_s} \left(\mathbf{s}^H \mathbf{s} + \mathbf{s}^H \mathbf{D V D s} - 2\Re \left\{ \mathbf{s}^H \mathbf{\Lambda D s} \right\} \right),$$

where $\boldsymbol{v}$, $\mathbf{\Lambda}$ and $\mathbf{V}$ are defined as

$$\boldsymbol{v}(f) = \left(e^{j2\pi f(N_1)}, \ldots, e^{j2\pi f(0)}, \ldots, e^{j2\pi f(N_2)} \right)^T,$$
$$\mathbf{I}_N = \int_{-\frac{1}{2}}^{\frac{1}{2}} \boldsymbol{v}(f) \boldsymbol{v}^H(f) \, df,$$
$$\mathbf{D} = \mathrm{diag}\left([N_1, \; N_1 + 1, \ldots, \; N_2 - 1, \; N_2] \right),$$
$$\mathbf{\Lambda} = j2\pi \int_{-\frac{1}{2}}^{\frac{1}{2}} f \boldsymbol{v}(f) \boldsymbol{v}(f)^H df,$$
$$\mathbf{V} = 4\pi^2 \int_{-\frac{1}{2}}^{\frac{1}{2}} f^2 \boldsymbol{v}(f) \boldsymbol{v}(f)^H df.$$

References

1. Woodward, P.M. *Probability and Information Theory with Application to Radar*; Artech House: Norwood, MA, USA, 1953.
2. Rihaczek, A.W. Delay-Doppler ambiguity function for wideband signals. *IEEE Trans. Aerosp. Electron. Syst.* **1967**, *3*, 705–711. [CrossRef]
3. Swick, D.A. *A Review of Wideband Ambiguity Functions*; Technical Report 6994; Naval Res. Lab.: Washington, DC, USA, 1969.
4. Trees, H.L.V. *Detection, Estimation, and Modulation Theory, Part III: Radar—Sonar Signal Processing and Gaussian Signals in Noise*; John Wiley & Sons: Hoboken, NJ, USA, 2001.
5. Mengali, U.; D'Andrea, A.N. *Synchronization Techniques for Digital Receivers*; Plenum Press: New York, NY, USA, 1997.
6. Trees, H.L.V. *Optimum Array Processing*; Wiley-Interscience: New York, NY, USA, 2002.
7. Ricker, D.W. *Echo Signal Processing*; Kluwer Academic; Springer: New York, NY, USA, 2003.
8. Chen, J.; Huang, Y.A.; Benesty, J. Time Delay Estimation. In *Audio Signal Processing for Next-Generation Multimedia Communication Systems*; Huang, Y., Benesty, J., Eds.; Springer: Boston, MA, USA, 2004; Chapter 8, pp. 197–227.
9. Levy, B.C. *Principles of Signal Detection and Parameter Estimation*; Springer: Berlin/Heidelberg, Germany, 2008.
10. Munoz, D.; Lara, F.B.; Vargas, C.; Enriquez, R. *Position Location Techniques and Applications*; Academic Press: Oxford, UK, 2009.
11. Yan, J.; Tiberius, C.C.J.M.; Janssen, G.J.M.; Teunissen, P.J.G.; Bellusci, G. Review of range-based positioning algorithms. *IEEE Trans. Aerosp. Electron. Syst.* **2013**, *28*, 2–27. [CrossRef]
12. Zavorotny, V.U.; Gleason, S.; Cardellach, E.; Camps, A. Tutorial on remote sensing using GNSS bistatic radar of opportunity. *IEEE Geosci. Remote Sens. Mag.* **2014**, *2*, 8–45. [CrossRef]
13. Trees, H.L.V.; Bell, K.L. (Eds.) *Bayesian Bounds for Parameter Estimation and Nonlinear Filtering/Tracking*; Wiley/IEEE Press: New York, NY, USA, 2007.

14. Trees, H.L.V. *Detection, Estimation, and Modulation Theory: Part I*; Wiley: New York, NY, USA, 1968.
15. Kay, S.M. *Fundamentals of Statistical Signal Processing: Estimation Theory*; Prentice-Hall: Englewood Cliffs, NJ, USA, 1993.
16. Stoica, P.; Nehorai, A. Performances study of conditional and unconditional direction of arrival estimation. *IEEE Trans. Acoust. Speech Signal Process.* **1990**, *38*, 1783–1795. [CrossRef]
17. Renaux, A.; Forster, P.; Chaumette, E.; Larzabal, P. On the High-SNR Conditional Maximum-Likelihood Estimator Full Statistical Characterization. *IEEE Trans. Signal Process.* **2006**, *54*, 4840 – 4843. [CrossRef]
18. Jin, Q.; Wong, K.M.; Luo, Z.Q. The estimation of time delay and Doppler stretch of wideband signals. *IEEE Trans. Signal Process.* **1995**, *43*, 904–916. [CrossRef]
19. Niu, X.X.; Ching, P.C.; Chan, Y. Wavelet based approach for joint time delay and Doppler stretch measurements. *IEEE Trans. Aerosp. Electron. Syst.* **1999**, *35*, 1111–1119. [CrossRef]
20. Dogandzic, A.; Nehorai, A. Cramér-Rao Bounds for Estimating Range, Velocity, and Direction with an Active Array. *IEEE Trans. Signal Process.* **2001**, *49*, 1122–1137. [CrossRef]
21. Noels, N.; Wymeersch, H.; Steendam, H.; Moeneclaey, M. True Cramér-Rao bound for timing recovery from a bandlimited linearly Modulated waveform with unknown carrier phase and frequency. *IEEE Trans. Commun.* **2004**, *52*, 473–483. [CrossRef]
22. He-Wen, W.; Shangfu, Y.; Qun, W. Influence of random carrier phase on true Cramer-Rao lower bound for time delay estimation. In Proceedings of the IEEE International Conference on Acoustics, Speech and Signal Processing (ICASSP), Honolulu, HI, USA, 15–20 April 2007.
23. Wei, H.; Ye, S.; Wan, Q. Influence of phase on Cramer-Rao lower bounds for joint time delay and Doppler stretch estimation. In Proceedings of the IEEE International Symposium on Signal Processing and Its Applications (ISSPA), Sharjah, UAE, 12–15 February 2007.
24. Johnson, J.; Fowler, M. Cramer-Rao lower bound on Doppler frequency of coherent pulse trains. In Proceedings of the IEEE International Conference on Acoustics, Speech and Signal Processing (ICASSP), Las Vegas, NV, USA, 31 March–4 April 2008.
25. Closas, P.; Fernández-Prades, C.; Fernández-Rubio, J.A. Cramér-Rao bound analysis of positioning approaches in GNSS receivers. *IEEE Trans. Signal Process.* **2009**, *57*, 3775–3786. [CrossRef]
26. Enneking, C.; Stein, M.; Castañeda, M.; Antreich, F.; Nossek, J.A. Multi-satellite time-delay estimation for reliable high-resolution GNSS receivers. In Proceedings of the IEEE/ION Position, Location and Navigation Symposium, Myrtle Beach, SC, USA, 23–26 April 2012.
27. Pourhomayoun, M.; Fowler, M. Cramer-Rao lower bound for frequency estimation for coherent pulse train with unknown pulse. *IEEE Trans. Aerosp. Electron. Syst.* **2014**, *50*, 1304–1312. [CrossRef]
28. Nan, Z.; Zhao, T.; Huang, T. Cramer-Rao lower bounds of joint time delay and Doppler-stretch estimation with random stepped-frequency signals. In Proceedings of the IEEE International Conference on Digital Signal Processing (DSP), Beijing, China, 16–18 October 2016.
29. Zhao, T.; Huang, T. Cramer-Rao Lower Bounds for the Joint Delay-Doppler Estimation of an Extended Target. *IEEE Trans. Signal Process.* **2016**, *64*, 1562–1573. [CrossRef]
30. Gogolev, I.; Yashin, G. Cramer-Rao Lower Bound of Doppler Stretch and Delay in Wideband Signal Model. In Proceedings of the IEEE Conference of Russian Young Researchers in EEE (EIConRus), St. Petersburg, Russia, 1–3 February 2017.
31. Chen, Y.; Blum, R.S. On the Impact of Unknown Signals on Delay, Doppler, Amplitude, and Phase Parameter Estimation. *IEEE Trans. Signal Process.* **2019**, *67*, 431–443. [CrossRef]
32. Medina, D.; Ortega, L.; Vilà-Valls, J.; Closas, P.; Vincent, F.; Chaumette, E. Compact CRB for Delay, Doppler, and Phase Estimation—Application to GNSS SPP and RTK Performance Characterisation. *IET Radar Sonar Navig.* **2020**, accepted for publication. [CrossRef]
33. Bartov, A.; Messer, H. Lower bound on the achievable DSP performance for localizing step-like continuous signals in noise. *IEEE Trans. Signal Process.* **1998**, *46*, 2195–2201. [CrossRef]
34. Yau, S.F.; Bresler, Y. A Compact Cramér-Rao Bound Expression for Parametric Estimation of Superimposed Signals. *IEEE Trans. Signal Process.* **1992**, *40*, 1226–1230. [CrossRef]
35. Ottersten, B.; Viberg, M.; Stoica, P.; Nehorai, A. Exact and Large Sample Maximum Likelihood Techniques for Parameter Estimation and Detection in Array Processing. In *Radar Array Processing*; Haykin, S., Litva, J., Shepherd, T.J., Eds.; Springer: Heidelberg, Germany, 1993; Chapter 4, pp. 99–151.

36. Menni, T.; Chaumette, E.; Larzabal, P.; Barbot, J. New Results on Deterministic Cramér–Rao Bounds for Real and Complex Parameters. *IEEE Trans. Signal Process.* **2012**, *60*, 1032–1049. [CrossRef]
37. Speiser, J.M. Wideband ambiguity functions. *IEEE Trans. Inf. Theory* **1967**, *13*, 122–123. [CrossRef]
38. Lin, Z.B. Wideband ambiguity function of broadband signals. *J. Acoust. Soc. Am.* **1988**, *83*, 2108–2116. [CrossRef]
39. Dawood, M.; Narayanan, R. Generalised wideband ambiguity function of a coherent ultrawideband random noise radar. *IEE Proc. Radar Sonar Navig.* **2003**, *150*, 379 – 386. [CrossRef]
40. Teunissen, P.J.G.; Montenbruck, O. (Eds.) *Handbook of Global Navigation Satellite Systems*; Springer: Cham, Switzerland, 2017.
41. Lestarquit, L.; Peyrezabes, M.; Darrozes, J.; Motte, E.; Roussel, N.; Wautelet, G.; Frappart, F.; Ramillien, G.; Biancale, R.; Zribi, M. Reflectometry With an Open-Source Software GNSS Receiver: Use Case With Carrier Phase Altimetry. *IEEE J. Sel. Top. Appl. Earth Obs. Remote Sens.* **2016**, *9*, 4843–4853. [CrossRef]
42. Cardellach, E.; Li, W.; Rius, A.; Semmling, M.; Wickert, J.; Zus, F.; Ruf, C.S.; Buontempo, C. First Precise Spaceborne Sea Surface Altimetry With GNSS Reflected Signals. *IEEE J. Select. Top. Appl. Earth Observ. Remote Sens.* **2019**, *13*, 102–112. [CrossRef]
43. Skolnik, M.I. *Radar Handbook*, 3rd ed.; McGraw-Hill: New York, NY, USA, 1990.
44. Das, P.; Vilà-Valls, J.; Chaumette, E.; Vincent, F.; Davain, L.; Bonnabel, S. On the Accuracy Limit of Time-delay Estimation with a Band-limited Signal. In Proceedings of the IEEE International Conference on Acoustics, Speech and Signal Processing (ICASSP), Brighton, UK, 12–17 May 2019.
45. Sussman, S. Least-square synthesis of radar ambiguity functions. *IRE Trans. Inf. Theory* **2009**, *8*, 246–254. [CrossRef]
46. Arlery, F.; Kassab, R.; Tan, U.; Lehmann, F. Efficient Gradient Method for Locally Optimizing the Periodic/Aperiodic Ambiguity Function. In Proceedings of the IEEE Radar Conference (RadarConf), Philadelphia, PA, USA, 2–6 May 2016.
47. Sebt, M.A.; Sheikhi, A.; Cheikhi, M.N. Orthogonal frequency-division multiplexing radar signal design with optimised ambiguity function and low peak-to-average power ratio. *IET Radar Sonar Navig.* **2009**, *3*, 122–132. [CrossRef]
48. Cavazzuti, M. *Optimization Methods: From Theory to Design Scientific and Technological Aspects in Mechanics*; Springer: Berlin/Heidelberg, Germany, 2012.
49. Dréao, J.; Chatterjee, A.; Pétrowski, A.; Siarry, P.; Taillard, E. *Metaheuristics for Hard Optimization: Methods and Case Studies*; Springer: Berlin/Heidelberg, Germany, 2006.
50. Fernández-Prades, C.; Lo Presti, L.; Falletti, E. Satellite radiolocalization from GPS to GNSS and beyond: Novel technologies and applications for civil mass market. *Proc. IEEE* **2011**, *99*, 1882–1904. [CrossRef]
51. Kaplan, E.D. (Ed.) *Understanding GPS: Principles and Applications*, 2nd ed.; Artech House: Norwood, MA, USA, 2006.